SCIENTIA BRUNEIANA

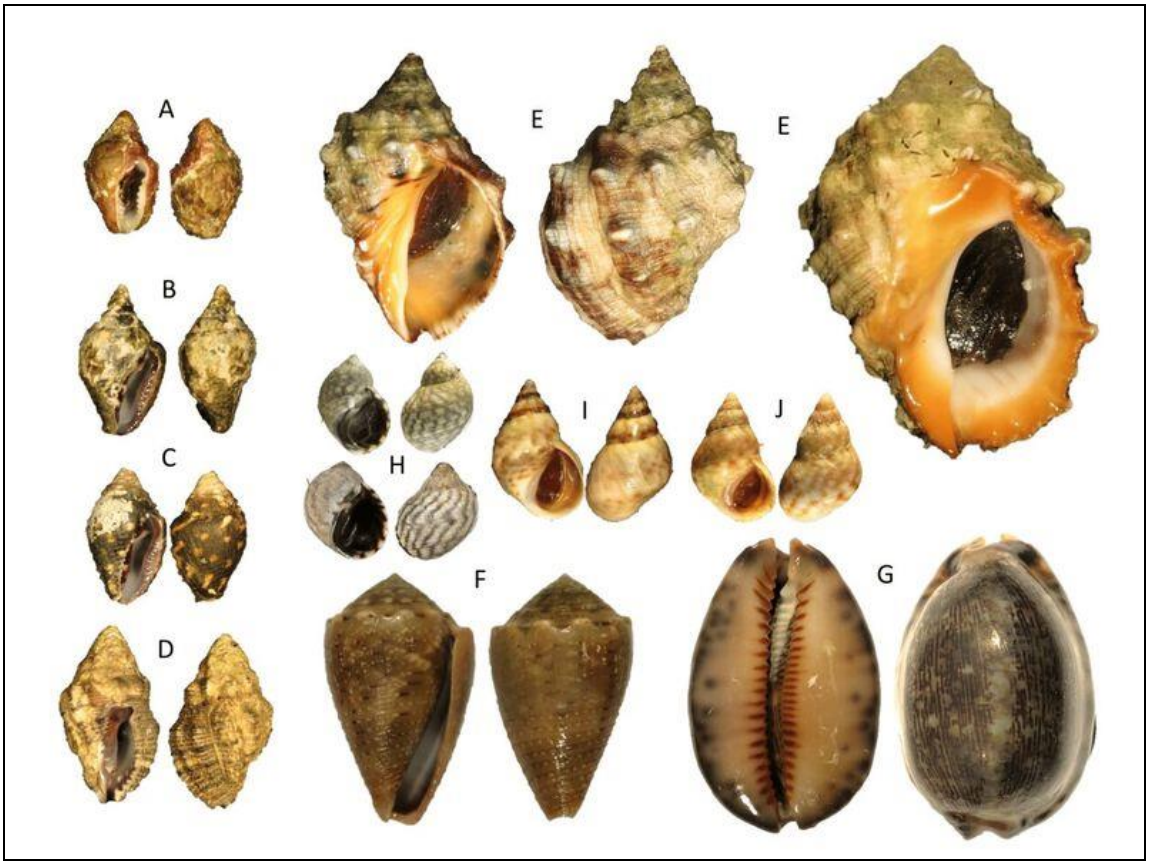

OFFICIAL JOURNAL OF
THE FACULTY OF SCIENCE
UNIVERSITI BRUNEI DARUSSALAM

ISSN : 1819-9550 (Print), 2519-9498 (Online) - Volume : 16(2), 2017

First Published 2017 by

Faculty of Science,
Universiti Brunei Darussalam
Jalan Tungku Link
Bandar Seri Begawan BE1410
Brunei Darussalam

This book consists of papers prepared by staff of Universiti Brunei Darussalam, and peer-reviewed by local and international referees.

Cataloguing in Publication Data

Scientia Bruneiana / Chief Editor Abby Tan Chee Hong

52 p. + iv; 30 cm

ISSN 2519-9498 (Online), ISSN 1819-9550 (Print)

1. Research – Brunei Darussalam. 2. Science – Brunei Darussalam

Q180.B7 B788 2017

Cover photo: Snail species collected at Pulau Punyit. (Courtesy: David J. Marshall, Azmi Aminuddin and Pg Saimon Pg Hj Ahmad).

Printed in Brunei Darussalam by
Educational Technology Centre,
Universiti Brunei Darussalam

mk

SCIENTIA BRUNEIANA
Vol. 16, No. 2

Greetings from the Dean of UBD's Faculty of Science.

I am pleased to introduce our second issue for 2017 which again highlights some important and significant findings made by our own researchers in the fields of the natural and applied sciences. This journal is unique as it does not focus solely on the fundamental sciences but also covers the applied sciences, thus promoting inter- and multi-disciplinarity.

The Faculty has a strong record of ground-breaking research in the biological, physical and mathematical sciences. The papers appearing in this issue demonstrate the ongoing commitment of our research staff to innovative science that contributes to the national interest as well as broadening the knowledge base of the global scientific community. The examples of collaborative research showcased here highlight the recognition that quality Bruneian research is now receiving across the world.

I am also pleased to note contributions from leading scientists in this issue. In our pursuit of international excellence and global recognition, we are certain this trend will continue.

I would like to thank my colleagues in the Faculty of Science, particularly the authors, associate and subject editors for their continuous support.

Yours Sincerely
Abby Tan Chee Hong
Chief Editor
Scientia Bruneiana

SCIENTIA BRUNEIANA

A journal of science and science-related matters published twice a year by the Faculty of Science, University Brunei Darussalam. Contributions are welcomed in any area of science, mathematics, medicine or technology. Authors are invited to submit manuscripts to the editor or any other member of the Editorial Board. Further information including instructions for authors can be found in the Notes to Contributors section (the last three pages).

EDITORIAL BOARD

SCIENTIA BRUNEIANA is published by the Faculty of Science,
Universiti Brunei Darussalam, Brunei Darussalam BE 1410

ISSN 2519-9498 (Online), ISSN 1819-9550 (Print)

1. Research – Brunei Darussalam. 2. Science – Brunei Darussalam

Q180.B7 B788 2017

SCIENTIA BRUNEIANA

Publication Ethics Policy

The Editorial Board of *Scientia Bruneiana* is committed to implementing and maintaining the publication standards of a high-quality peer-reviewed scientific journal.

Each manuscript submitted to *Scientia Bruneiana* is examined by a referee with recognised expertise in the manuscript's subject area, and all communications between the referee and the author(s) pass must first through the Editorial Board, so that the identity of the referee remains confidential.

No one will be appointed as the referee of a manuscript if he or she is known to have a potentially compromising relationship with one or more of the authors of the manuscript, as for example in being related through blood or marriage to an author, or in being the research supervisor or research student of an author.

The Editorial Board of *Scientia Bruneiana* makes every effort to ensure that each paper published in the journal is free of plagiarism, redundant or recycled text, and fabricated or misrepresented data. Where possible, plagiarism detection software will be used to check for plagiarised or recycled text.

Provided that a manuscript is free of the ethical lapses described in the previous paragraph, the decision to publish it in *Scientia Bruneiana* is based entirely on its scientific or academic merit, as judged by the referee. The referee's assessment of the merit of the manuscript is final. While a full statement of the reasons behind the referee's decision will be passed on to the author(s), no appeals from the author(s) will be entertained.

Under no circumstances will the referee of a paper published in *Scientia Bruneiana* be credited as one of the authors of the paper, and other papers that have been authored or co-authored by the referee will be admitted to the paper's list of references only after an independent third party with expertise in the area has been consulted to ensure that the citation is of central relevance to the paper.

If a member of the Editorial Board of *Scientia Bruneiana* is listed as an author of a manuscript submitted to *Scientia Bruneiana*, that Board member will play no part whatsoever in the processing of the manuscript.

Where necessary, any corrections or retractions of papers previously published in *Scientia Bruneiana* will be printed in the earliest possible edition of the journal, once the need for a correction or retraction has been drawn to the attention of the Editorial Board.

SCIENTIA BRUNEIANA VOL. 16, NO. 2

2017

Table of Contents **Page Numbers**

Large-scale and uniform fabrication of anodic TiO_2 nanotubes at the inner surface of high-aspect-ratio Ti tubes

*Chengjie Xiang[1] and Lidong Sun[1]**

[1]State Key Laboratory of Mechanical Transmission, School of Materials Science and Engineering, Chongqing University, Chongqing 400044, PR China

**corresponding author email: lidong.sun@cqu.edu.cn*

Because of their high specific strength and superior corrosion resistance, titanium and its alloys have been widely used in aerospace, navigation, desalination, automotive and petroleum industries. Titanium tubes and pipes are of particular interest for heat and mass transfer in heat exchangers in these fields. However, a few critical problems are currently concerned: the frictional drag at the solid/liquid interface and the fouling that lowers the heat transfer coefficient.[1] A superhydrophobic coating developed at the inner and/or outer surface of a tube is capable of providing drag reduction, suppressing fouling formation, and producing condensation heat transfer, therefore enhances the performance of heat exchangers.[2-6] Nevertheless, it remains a great challenge to fabricate such superhydrophobic coatings on tubular substrates, especially at their inner surfaces considering the partially opened geometrical feature.

Anodic oxidation of titanium and its alloys enables the formation of highly ordered TiO_2 nanotubes, which have attracted growing interest in the fields of solar cells,[7-10] photocatalysis,[11] drug delivery,[12] lithium-ion batteries,[13] and so on. Wetting property of the TiO_2 nanotubes can be well tailored by controlling their structures and employing organic molecules of low surface energy. They are thus competent as the superhydrophobic coatings mentioned above. Nonetheless, the existing methods are unsuitable for large-scale and mass production of uniform TiO_2 nanotubes on tubular substrates.

Sun and co-workers[14] systematically studied the effect of electrode deployment on the formation of TiO_2 nanotubes, as shown in ***Figure 1***. A conventional planar cathode was used. The results reveal that nanotubes are formed at both surfaces of a titanium tubular electrode, regardless of the deployment. When the anode is dipped into electrolyte solution (about 17 mm immerged) and set perpendicular to the liquid surface (see ***Figure 1a***), the nanotube length exhibits an almost linear decrease from the tube bottom to top at the inner surface (see ***Figure 1d***). This is attributed to the limited diffusion pathway available only from tube bottom for F^- ions. When the anode is completely immerged into the electrolyte solution while kept parallel to the liquid surface and the cathode (see Figure 1b), the nanotube length decreases gradually from tube mouth at both ends to the middle part, as exhibited in ***Figure 1e***. This is due to the situation that the F^- ions can diffuse into the tube from either side. In a similar case where the anode is set perpendicular to the cathode (Figure 1c), the nanotube length decreases progressively from the end near the cathode to the other end, as shown in ***Figure 1f***. In all of the experimental setups, at the outer substrate surface the nanotube length decreases gradually from the part close to the cathode to that far away, because of the potential drop in the organic electrolyte solution.[15,16] This study indicates that it is difficult to coat either inner or outer surface of a Ti tube with uniform TiO_2 nanotube arrays using conventional anodization scheme.

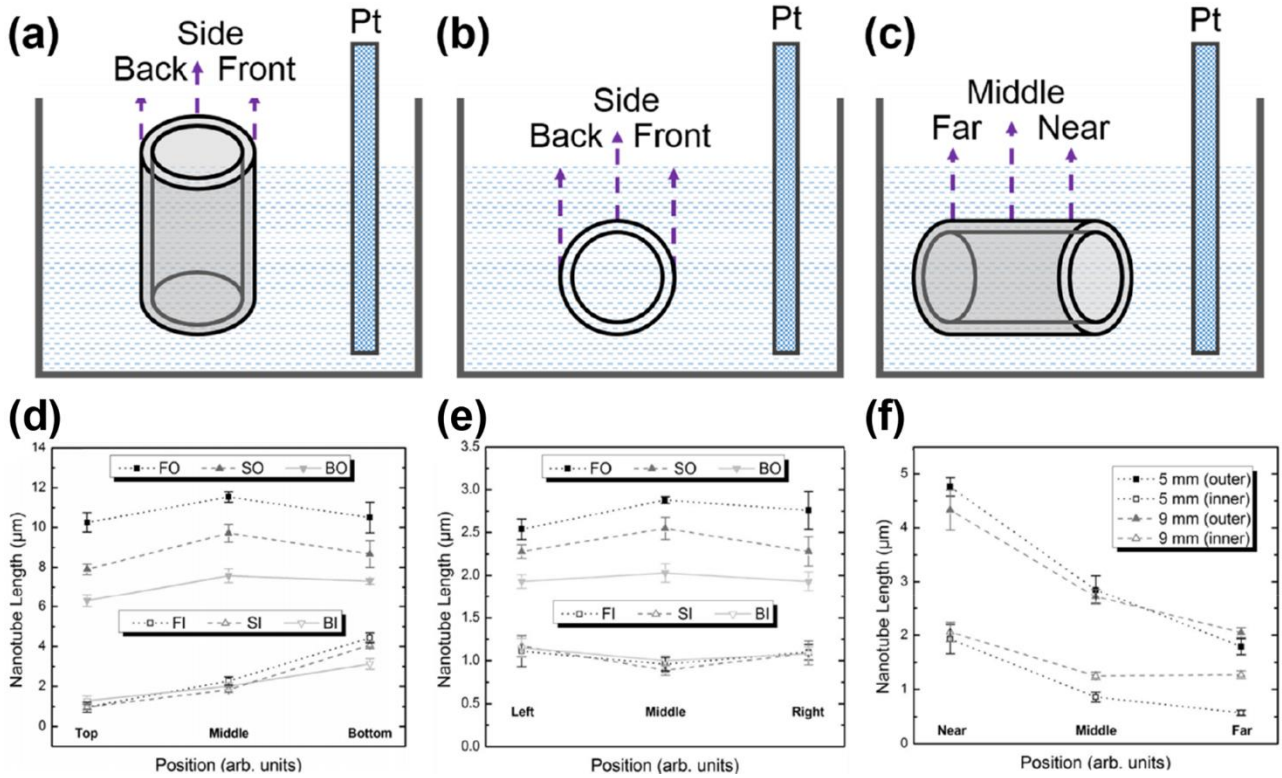

Figure 1. Schematic illustration of different electrode deployments, where a planar cathode is used with the tubular anode being: (a) perpendicular to the liquid surface and parallel to the cathode, (b) immersed in the solution and parallel to the cathode, and (c) immersed in the solution and perpendicular to the cathode. Corresponding length of TiO_2 nanotubes at both inner and outer surfaces is given below each illustration in (d), (e) and (f), respectively. Reprinted with permission from L. Sun, *et al.*, *Langmuir* 30 (10), 2835-2841. Copyright © 2014 American Chemical Society.

The key to control the nanotube uniformity is to ensure a uniform distribution of electric field along the radial and axial directions. To this end, Xiang and co-workers[5] designed a coaxial electrochemical anodization, as illustrated in ***Figure 2a***. In this setup, a titanium tube is employed as the anode while a stainless steel wire is used as the cathode, where the substrate itself also performs as a container to accommodate electrolyte solution. With this method, uniform TiO_2 nanotube arrays are produced at the inner surface of Ti tubes with a dimension of 1000 mm in length and 10 mm in diameter (aspect ratio: 100), as displayed in ***Figure 2b***. This is in good contrast to the non-uniform nanotubes yielded with conventional deployments in ***Figure 1***, though with much smaller substrates (aspect ratio: <6). A length limit of about 1 μm exists for the nanotubes, as a result of limited electrolyte volume confined inside the tubular compartment. The coaxial electrochemical anodization can be applied to longer substrates and also other valve metals suitable for anodic oxidation. However, it is further found that once the substrate diameter drops to a very low regime, e.g., 3 mm, the nanotubes become non-uniform again and even are absent at certain regions. This is ascribed to the limited volume rendered by the small tubes. Bubbles that are released in the process of anodization are adsorbed to the inner surface, accumulate and eventually expel the electrolyte solution out of the tubular compartment.

In application of microfluids and microelectronics, slim tubes of small diameters have been frequently used. In this regard, Wang and co-workers[6] further developed a coaxial anodic oxidation under dynamic electrolyte conditions, as sketched in ***Figure 3a***. In this setup, the flowing electrolyte is adopted to make up the solution, drive out the bubbles, and also cool down the system. The growth of TiO_2 nanotubes is closely related to the electrolyte

flow rate. When the flow rate is too low, the nanotube growth rate is limited. The problem still remains. When the flow rate is too high, the nanotubes are able to fully cover the inner surface, whereas the length increases from substrate bottom to the top. This is because fresh electrolyte flows into the tubular compartment at the bottom part, where the fluoride concentration is high. This leads to an enhanced etching rate to the already-formed TiO_2 nanotubes by chemical dissolution and hence shorter nanotubes close to the inletting end.[17] Consequently, the length at the inner surface is tailorable by controlling the electrolyte flow rate. Accordingly, uniform coatings of TiO_2 nanotubes are attained using Ti tubes of 930 mm in length and 3 mm in diameter (aspect ratio: 310), as shown in ***Figure 3b***.

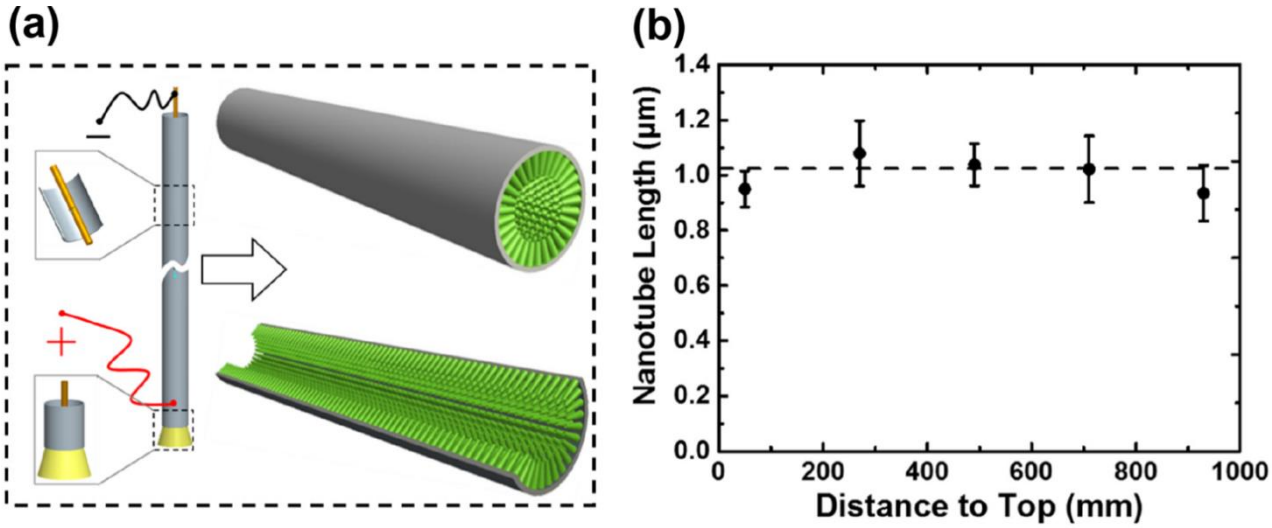

Figure 2. (***a***) Schematic illustration of coaxial electrochemical anodization; (***b***) Length of TiO_2 nanotubes at the inner surface of Ti tubes examined along the axial direction. Adapted with permission from C. Xiang, *et al.*, *J. Phys. Chem. C* 121 (28), 15448-15455. Copyright © 2017 American Chemical Society.

The above coatings of TiO_2 nanotubes are intrinsically hydrophilic, and can be further tailored to be superhydrophobic with a water contact angle of over 160° and sliding angle of below 3°, with judiciously designed structure. It is thus promising for applications in drag reduction, condensation heat transfer, antifouling, and so on.

The coaxial electrochemical anodization can also be extended to the outer tube surface, and even to both surfaces anodized simultaneously. In the latter case, the uniformity control becomes more difficult. The asymmetric deployment between the anode and cathode results in different oxidation and dissolution processes, which should be taken into account to ensure uniform nanotubes.

Acknowledgements

We acknowledge the financial support from the National Natural Science Foundation of China (No. 51501024), the Chongqing Research Program of Basic Research and Frontier Technology (No. cstc2015jcyjA90004), and the Fundamental Research Funds for the Central Universities (No. 106112016CDJZR135506).

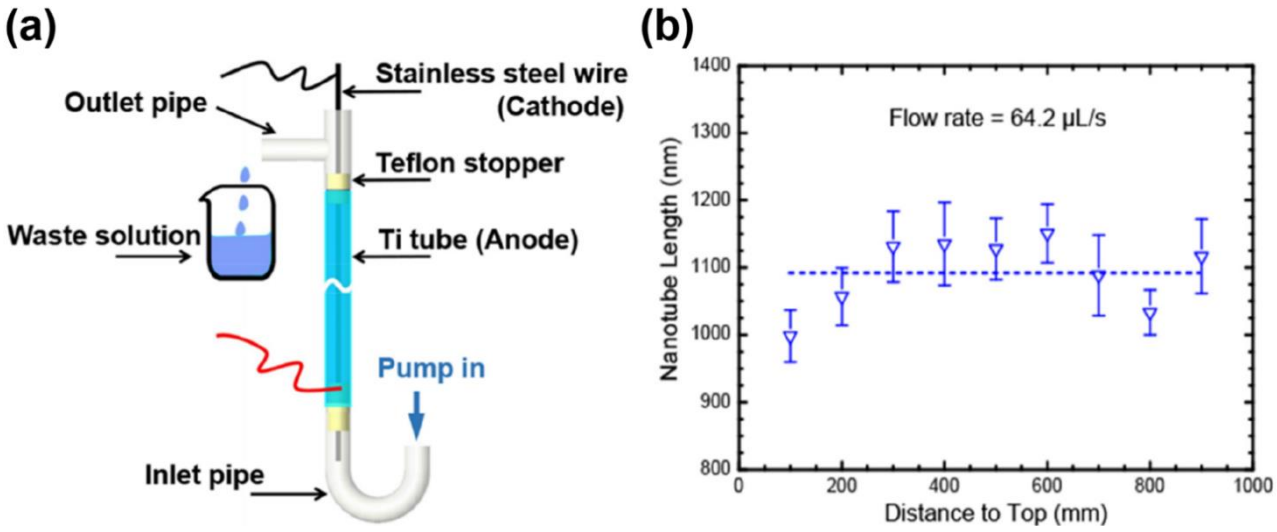

Figure 3. (***a***) Schematic illustration of coaxial electrochemical anodization with flowing electrolyte; (***b***) Length of TiO_2 nanotubes at the inner surface of Ti tubes examined along the axial direction. Reprinted from *Corros. Sci.*, Volume 124, Y. Wang, *et al.*, Coaxial anodic oxidation under dynamic electrolyte conditions for inner surface patterning of high-aspect-ratio and slim Ti tubes, 193-197. Copyright ©2017, with permission from Elsevier.

References

[1] Y. C. Jung and B. Bhushan, *J. Phys.: Condens. Matter*, **2010**, 22, 035104.

[2] N. Miljkovic, *et al.*, *Nat. Commun.*, **2013**, 4, 2517.

[3] N. Miljkovic, *et al.*, *Nano Lett.*, **2013**, 13(1), 179-187.

[4] F. Y. Lv, and P. Zhang, *Energy Convers. Manage*, **2016**, 113, 165-176.

[5] C. Xiang, *et al.*, *J. Phys. Chem. C*, **2017**, 121(28), 15448-15455.

[6] Y. Wang, *et al.*, *Corros. Sci.*, **2017** 124, 193-197. https://doi.org/10.1016/j.corsci.2017.04.029

[7] L. Sun, *et al.*, *Energy Environ. Sci.*, **2011**, 4(6), 2240-2248. http://dx.doi.org/10.1016/j.electacta.2016.03.099

[8] X. Zhao, *et al.*, *Electrochim. Acta*, **2016**, 199, 180-186.

[9] L. Sun, *et al.*, *J. Nanosci. Nanotechnol.*, **2014**, 14(2), 2050-2064.

[10] L. Sun, *et al.*, *Nanosci. Nanotechnol. Lett.*, **2012**, 4(5), 471-482.

[11] A. Ghicov, *et al.*, *Nano Lett.*, **2006**, 6(5), 1080-1082.

[12] Y.-Y. Song, *et al.*, *J. Am. Chem. Soc.*, **2009**, 131(12), 4230-4232.

[13] Y. Tang, *et al.*, *Adv. Mater.*, **2014**, 26(35), 6111-6118.

[14] L. Sun, *et al.*, *Langmuir*, **2014**, 30(10), 2835-2841.

[15] L. Sun, *et al.*, *J. Electroanal. Chem.*, **2009**, 637(1-2), 6-12.

[16] L. Sun, *et al.*, *Langmuir*, **2010**, 26(23),18424-18429.

[17] L. Sun, *et al.*, *ChemPhysChem*, **2011**, 12(18), 3634-3641.

Removal of acid blue 25 from aqueous solution by using common salts and seawater to induce the salting out effect

Muhammad Raziq Rahimi Kooh[1], Muhammad Khairud Dahri[1], Linda B. L. Lim[1] and Lee Hoon Lim[1]*

[1]Chemical Sciences, Faculty of Science, Universiti Brunei Darussalam, Jalan Tungku Link, Gadong, Negara Brunei Darussalam

**corresponding author email: chernyuan@hotmail.com*

Abstract

This study used common salts (monovalent and divalent salts) and seawater to cause aggregation of an acid dye, AB25 to a particle size large enough to be removed by simple filtration using a filter paper. All the common salts ($CaCl_2$, $Mg(NO_3)_2$, KNO_3, KCl, NaCl) were able to produce high removal efficiencies of AB25 (100 mg/L, unadjusted pH) at 99.4%, 90.3%, 98.4%, 99.3% and 99.3%, respectively, while a 2.5x dilution of seawater was successful in removing up to 93.8% of AB25. These findings proved the effectiveness of this method which is a much simpler and direct approach to dye wastewater remediation.

Index Terms: Acid blue 25, dye aggregation, ionic strength, seawater, salting-out effect

1. Introduction

In the past, all the dye materials were obtained from natural sources which include root, flower, barks, insects and minerals.[1] These practices gradually declined after the accidental discovery of the first synthetic dye in 1856, as the shift from natural to synthetic source make more economic sense for the thriving industrialising nations at that time.[1] Because of the vibrant colour, chemical and thermal stability of synthetic dyes, dye wastewater has become an environmental liability as its untreated form when discharged to rivers has devastating effects and is known to completely destroy an aquatic habitat,[2] and it may also seep into groundwater and contaminate potable water source.

The synthetic dyes are further classified into several categories depending on their chemical structures and functional groups. Some of the major dye classes are basic dyes (triphenylmethane and thiazine dyes), acid dyes (Ponceau S and acid blue 25), reactive dyes (reactive orange 16 and reactive blue 19), direct dyes (congo red, direct blue 71) and azo dyes (pigment yellow 12 and Brilliant Scarlet 3R). There are many methods of treating dye wastewater. Some of the examples include phytoremediation,[3,4] reverse osmosis, electrolysis, chemical degradation, adsorption and others;[5,6] however each method has its own advantages and disadvantages.

Reverse osmosis is high in operating cost, and the removal efficiency depends on the type of membrane material and pore size.[7] It was reported that membrane used for removing basic dyes may not perform the same way with acid dye.[7] Another disadvantage of the reverse osmosis is the resultant of a concentrated effluent.[5,6] Chemical degradation uses either oxidising or reducing agents which are not low-cost and it can result in mineralisation.[5] In addition, the degraded products can sometimes be more toxic than its original forms.[8] Adsorption method is one of the most researched methods due to its low cost and ease of usage. However the efficiency of adsorption depends on the adsorbent type. Our past studies involving agro-waste materials (e.g. Tarap fruit waste) and plant biomasses (water fern, *Nepenthes* leaves, *Casuarina* plant parts) were highly effective in treating basic dyes particularly the triphenylmethane dye class (e.g. methyl violet

2B, rhodamine B). However with the acid dye, the removal efficiency was much lower.[9-14] The maximum adsorption capacity reported for the removal of methyl violet 2B using *Azolla pinnata*,[14] soya bean waste,[15] *Nepenthes* leaves[9] and tarap fruit waste[11] were 199.4, 180.7, 194 and 263.7 mg/g, respectively, while the removal of acid blue 25 (AB25) using *Azolla pinnata* and soya bean waste were 50.5 and 38.4 mg/g, respectively.[13]

The aim of this research work is to investigate an alternative method for the removal of a selected acid dye (AB25) from aqueous solution by using a low-cost and sustainable method. Briefly, acid dye is one of the major classes of dye with wide applications in textile and cosmetic industries. The AB25 was chosen as the model acid dye for this experiment due to its harmfulness to the environment and it is also a very commonly studied acid dye. In this study, we proposed the use of seawater and various salts to cause aggregation of AB25 in aqueous solution. The proposed method is based on the concept of protein purification by the salting out effect, where salt concentration is increased which led to the decreased solubility of the protein.[16] The general explanation of this effect is that the high salt concentration allows more salt ions to interact with the water molecules, thus reducing the interaction of water molecules with the charged part of the protein, thereby leading to more protein-protein interactions.[17]

As for the case of the dye, the increase in the concentration of salts leads to the reduction of the thickness of the electric double layer surrounding the dye molecules. This forces the dye molecules to move closer to each other and provides higher probability of the molecules overcoming the electric force that keeps them apart.[18] In our previous study, we achieved a great success with a direct dye (direct blue 71) with a removal efficiency of 93% using a 40 times diluted seawater.[19]

The objectives of this study include studying the effects of various concentrations of monovalent salts, divalent salts and various dilutions of seawater on the aggregation and removal of AB25 dyes from aqueous solution.

2. Experimental

2.1 Sample preparation and chemicals

Acid blue 25 (AB25) ($C_{20}H_{13}N_2NaO_5S$, M_r 416.38 g/mol, 45% dye content, Sigma-Aldrich) was used without further purification. The salts (NaCl, KCl, KNO_3, $Mg(NO_3)_2$ and $CaCl_2$) (analytical grade) were obtained from BDH limited.

The seawater was collected from the Tungku Beach along the Muara-Tutong Highway in the Brunei-Muara District, Brunei Darussalam. The seawater was subjected to filtration using a Whatman No.1 filter paper to remove sand and other particles and the filtrate was then kept in an amber glass container away from sunlight.

2.2 Procedures for the aggregation of acid dye

A stock solution of 500 mg/L AB25 was first prepared, followed by preparing various concentrations of the salt solutions ranging from 0.001 M to 1.0 M. A total of 2 mL of the 500 mg/L AB25 was first transferred to a glass vial (final concentration of AB25 is 100 mg/L), followed by addition of distilled water with the salt added last whereby the total final volume of dye-salt mixture was 10 mL. The vials containing the dye-salt mixture were sealed using screw caps, hand-shaken and left to stand for 24 h. Duplicate were carried out for each salt. Similar procedures as mentioned above were used to investigate the effect of various dilutions of seawater on aggregation of AB25. After 24 h of standing, the dye-salt mixture was filtered using a Whatman filter paper No 1, and the filtrates were analysed at wavelength of 597 nm using a Shimadzu UV-1601PC UV–visible spectrophotometer.

Removal efficiency (RE) was calculated based on the following equation,

$$\mathrm{RE} = \frac{(C_i - C_f) \times 100\,\%}{C_i} \qquad (1)$$

where C_i is the initial dye concentration while C_f is the final dye concentration.

2.3 Surface morphology analysis

The aggregated dye obtained from the seawater treatment were collected, transferred to a glass petri-dish and dried in a desiccator. The dried sample was subjected to surface morphology analysis using a Tescan Vega XMU scanning electron microscope (SEM). The sample was gold-coated for 30 sec using a SPI-MODULE™ Sputter Coater.

3. Results and Discussions

3.1 Effect of different concentrations of salts and seawater on AB25 aggregation

Not all acid dyes can form dye aggregates. For the dye to be able to aggregate, the dye needs to possess a positively charged amine group at the position which can interact with the negatively charged sulphonate anion group of another dye molecule without causing any steric hindrance.[20] The molecular structure of AB25 is as shown in ***Figure 1a***, while ***Figure 1b*** shows the possible interaction between the sulphonate group of one AB25 and the $–NH_2$ group of another AB25 molecule.[21]

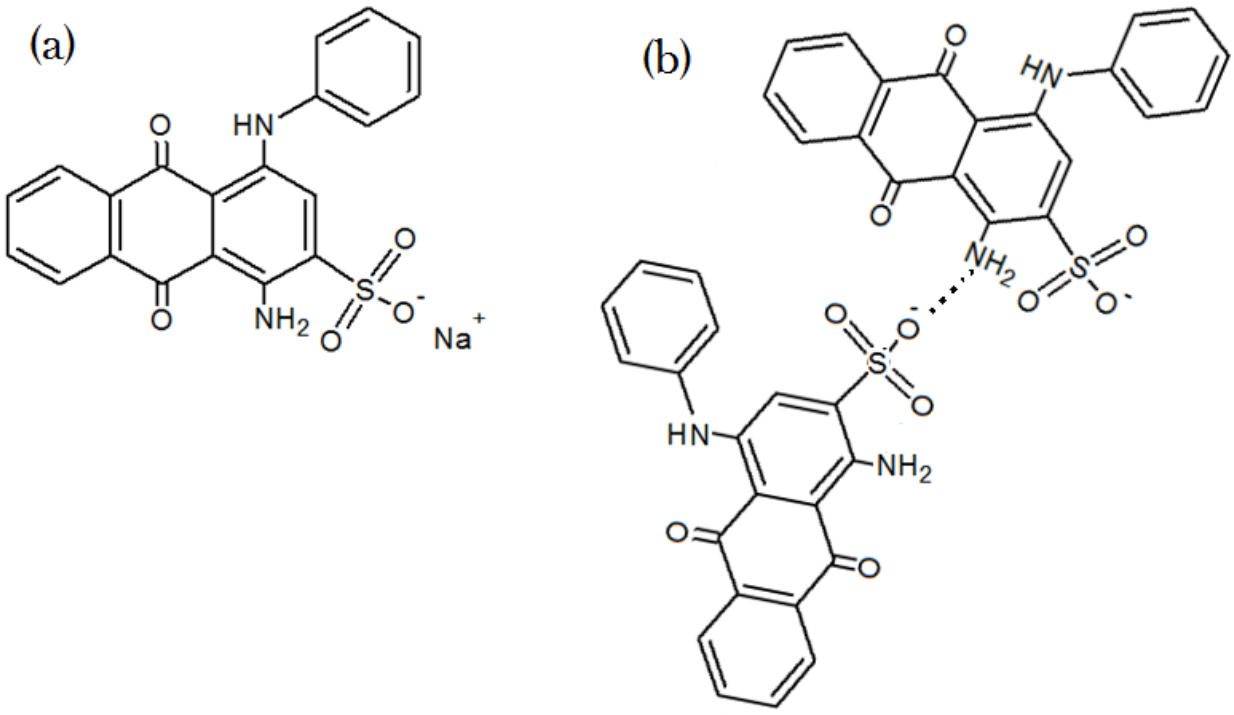

Figure 1. (***a***) a typical depiction of the molecular structure of AB25 dye (***b***) possible interaction between two AB25 molecules.

Figure 2 summarises the REs of AB25 (unadjusted pH, 100 mg/L dye) from aqueous solution by using various concentrations of monovalent and divalent salts. It can be observed that the increase of salt concentrations leads to the increase of the RE of AB25. At $CaCl_2$ concentrations of 0.01 M and 0.1 M, the RE values increased rapidly at 53.6% and 83.7%, respectively. Beyond 0.1 M $CaCl_2$, there was a slower increase in RE, where the maximum was achieved at 99.4% at 1 M $CaCl_2$. A similar pattern of the increase in RE was observed for the other divalent salt, $Mg(NO_3)_2$, but the RE was lower and peaked at 90.3%. The aggregated AB25 using $Mg(NO_3)_2$ was also observed to be very fine particles as compared to those obtained using $CaCl_2$ and other monovalent salts and they were able to pass through the Whatman No.1 filter paper. Similar patterns of the increase of RE were also observed with the increase in

concentration of the monovalent salts (KNO_3, KCl and NaCl), where their maximum REs were at 98.4%, 99.3% and 99.3%, respectively. When comparing among the three studied monovalent salts, NaCl was not as effective as KNO_3 and KCl salts and it requires a higher concentration to achieve the same level of RE. Comparing between the divalent and monovalent salts, $CaCl_2$ was able to achieve higher RE at lower salt concentration when compared to the other salts. This may be due to the capability of divalent cations to neutralise the charge of the dye aggregate more effectively (when compared to monovalent salts) and reducing the electrical forces keeping particles apart and allow easier agglomeration[22].

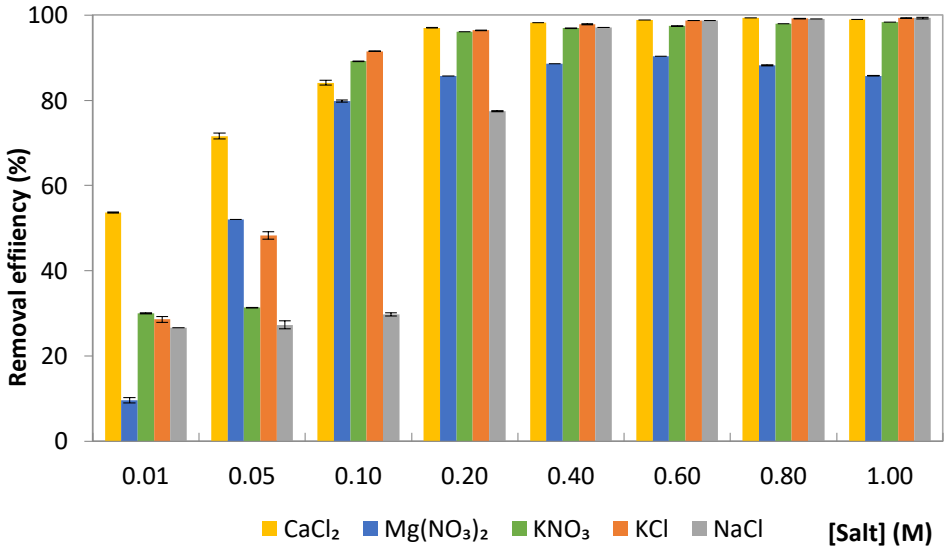

Figure 2. Removal efficiencies of AB25 (unadjusted pH, 100 mg/L dye) from aqueous solution by using various concentrations of monovalent and divalent salts.

The REs of 100 mg/L AB25 using various dilutions of seawater are as shown in ***Figure 3*** which shows a decrease in RE with increasing dilution of the seawater. A dilution factor (DF) of more than 50 did not result in significant removal of AB25 while the DF at 50x, 40x and 30x resulted in RE at 13.0%, 14.1% and 15.3 %, respectively. DF at 12.5x resulted in significant increase with RE at 46.5%. DF at 5x and 2.5x produced high RE at 89.0% and 93.8%, respectively. These data indicate that 1 part seawater can be added to 4 parts dye wastewater and yet achieve high removal efficiency. The high efficiency of seawater is most likely due to its high ionic strength that leads to the aggregation of AB25 to a particle size that can be easily filtered. Another possibility is the presence of trivalent cations in seawater, such as Fe(III) and Al(III), that are known to be more effective as coagulants than monovalent cations up to 1000 times.[22] Therefore the combination of all monovalent, divalent and trivalent salts in the seawater may enhance the overall process.

Comparing our proposed salting out method with other water treatment methods (photolysis, redox mediator and adsorption) as reported in the literatures the RE of using direct UV irradiation of AB25 (100 mg/L dye, pH 5.7) was estimated to be around 90%, however decolourisation reached 100% when H_2O_2 was added.[23] The uses of redox mediators (laccases derived from fungal sources: *Myceliophthora thermophilia*, *Polyporus pinisitus* and *Trametes versicolor*) (20 mg/L dye, pH 5.5) reported RE at 53.3%, 59.8% and 88.4%, respectively.[24] The adsorption of AB25 using *Azolla pinnata* (100 mg/L dye, pH 2.0)[13] and diatomite (100 mg/L dye, pH 2.0)[25] obtained RE at 40.8% and 60.0%, respectively. In summary, by using seawater method the RE is on par with the photolysis method (direct UV irradiation), but it performs better than the redox mediator and adsorption methods.

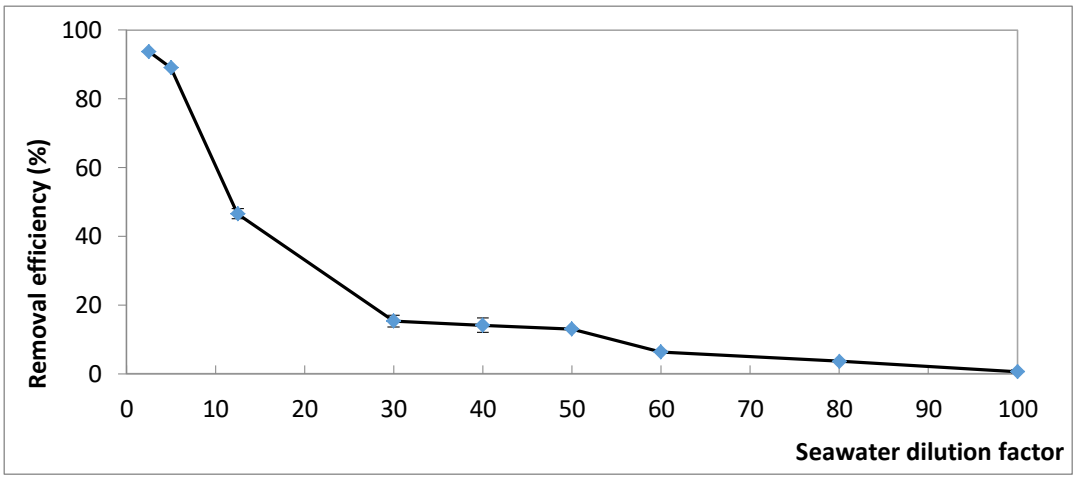

Figure 3. Removal of AB25 from aqueous solution using various dilutions of seawater.

3.2 Surface morphology analysis

Surface morphology analysis was carried out to characterise the aggregated AB25 (using seawater) collected on the filter paper as shown in ***Figure 4***. The SEM image, as shown in ***Figure 5***, helps to provide visualisation of the sample at higher magnification and resolution. The aggregated AB25 was observed to be irregular without definite shape and the surface appeared to be rough and folded. The mechanism for the formation of this structure is not known and is outside the scope of this study.

4. Conclusion.

This study used common salts and seawater to cause aggregation of AB25 to particle size large enough to be removed by simple filtration using filter paper. All the salts and seawater were able to produce high removal efficiencies proving that this method is effective and also a much simpler approach as compared to other methods as mentioned above.

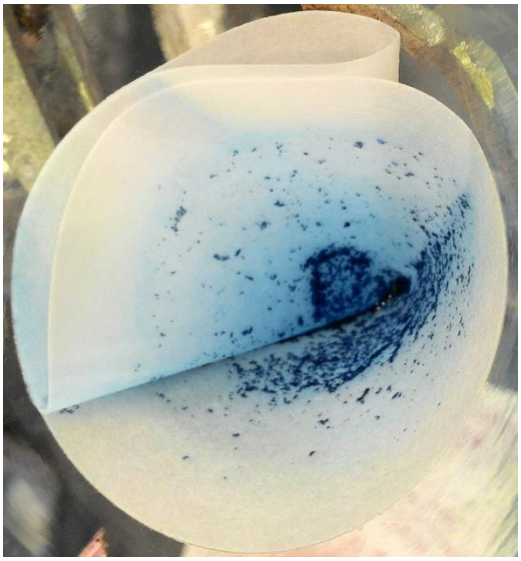

Figure 4. Aggregated dye obtained using seawater was collected on a filter paper.

Acknowledgements

The authors acknowledge the Government of Negara Brunei Darussalam and the Universiti Brunei Darussalam for their continuous support and Centre for Advanced Material and Energy Sciences (CAMES) of Universiti Brunei Darussalam for the usage of XRF machine.

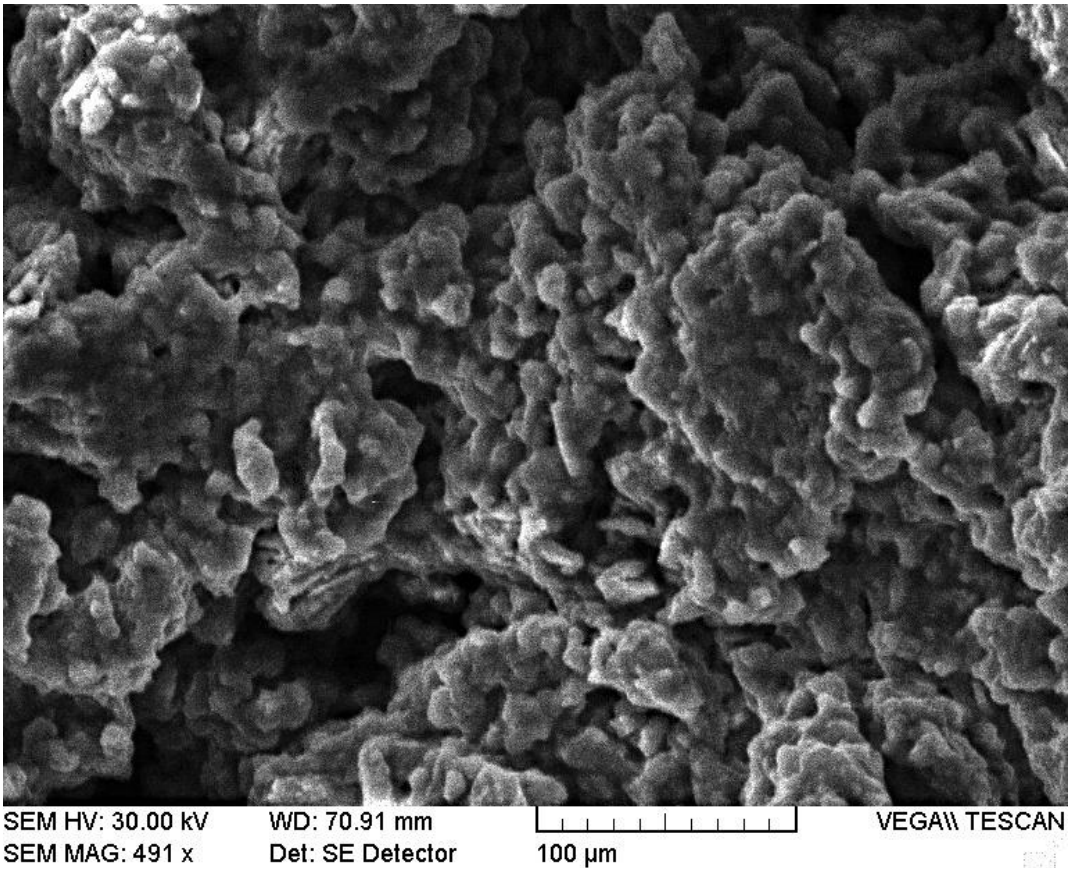

Figure 5. SEM image of the aggregated AB25 obtained using seawater under magnification of 491x.

References

[1] S. Saxena and A. S. M. Raja, Natural Dyes: Sources, Chemistry, Application and Sustainability Issues. In: S. S. Muthu (ed) Roadmap to Sustainable Textiles and Clothing: Eco-friendly Raw Materials, Technologies, and Processing Methods, **2014**, 37-80, Springer Singapore, Singapore.

[2] M. R. R. Kooh, M. K. Dahri and L. B. L. Lim, *Cogent Environ. Sci.*, **2016**, 2, 1140553.

[3] M. R. R. Kooh, L. B. L. Lim, L. H. Lim and M. K. Dahri, *J. Environ. Biotechnol. Res.*, **2016**, 5, 10-17.

[4] M. R. R. Kooh, L. B. L. Lim, L. H. Lim and O. A. Malik, *Int. J. Phytoremediation*, **2017**, Doi: 10.1080/15226514.2017.1365337.

[5] B. Volesky, *Hydrometallurgy*, **2001**, 59, 203-216.

[6] T. Robinson, G. McMullan, R. Marchant and P. Nigam, *Bioresour. technol.*, **2001**, 77, 247-255.

[7] L. Tinghui, T. Matsuura and S. Sourirajan, *Ind. Eng. Chem. Prod. Res. Dev.*, **1983**, 22, 77-85.

[8] C. Wang, A. Yediler, D. Lienert, Z. Wang and A. Kettrup, *Chemosphere*, **2003**, 52, 1225-1232.

[9] M. R. R. Kooh, M. K. Dahri and L. B. L. Lim, *Appl. Water Sci.*, **2017**, 7, 3859-3868.

[10] M. K. Dahri, M. R. R. Kooh and L. B. L. Lim, *J. Environ. Biotechnol. Res.*, **2017**, 6, 34-42.

[11] M. R. R. Kooh, M. K. Dahri and L. B. L. Lim, *Appl. Water Sci.*, **2017**, 7, 3573–3581.

[12] M. R. R. Kooh, M. K. Dahri and L. B. L. Lim, *J. Environ. Biotechnol. Res.*, **2016**, 4, 7-16.

[13] M. R. R. Kooh, M. K. Dahri, L. B. L. Lim and L. H. Lim, *Arabian J. Sci. Eng.*, **2015**, 41, 2453-2464.

[14] M. R. R. Kooh, L. B. L. Lim, M. K. Dahri, L. H. Lim and J. M. R. Sarath Bandara, *Waste and Biomass Valorization*, **2015**, 6, 547-559.
[15] M. R. R. Kooh, M. K. Dahri, L. B. L. Lim, L. H. Lim and O. A. Malik, *Environ. Earth Sci.*, **2016**, 75, 783.
[16] T. Arakawa and S. N. Timasheff, *Biochem.*, **1984**, 23, 5912-5923.
[17] R. K. Scopes, Separation by Precipitation. In: R. K. Scopes (ed) Protein Purification: Principles and Practice, **1994**, 71-101, Springer, New York.
[18] M. M. Clark, Transport modeling for environmental engineers and scientists, **2011**, John Wiley & Sons: New York.
[19] M. R. R. Kooh, D. Muhammad Khairud, L. B. L. Lim and L. H. Lim, *J. Environ. Biotechnol. Res.*, **2017**, 6, 53-57.
[20] Q. A. Acton, Issues in Materials and Manufacturing Research 2013 Edition, **2013**, Scholarly Editions: Atlanta.
[21] T. Nogrady and D. F. Weaver, Medicinal chemistry: a molecular and biochemical approach, 3rd Ed, **2005**, Oxford University Press.
[22] C. Binnie, M. Kimber and G. Smethurst, Basic water treatment, 3rd Ed, **2002**, Royal Society of Chemistry: Cambridge, UK.
[23] H. Ghodbane and O. Hamdaoui, *Chem. Eng. J.*, **2010**, 160, 226-231.
[24] H. Claus, G. Faber and H. König, *Appl. Microbiol. Biotechnol.*, **2002**, 59, 672-678.
[25] K. Badii, F. D. Ardejani, M. A. Saberi and N. Y. Limaee, *Indian J. Chem. Technol*, **2010**, 17, 7-16.

Molecular dynamics study of diffusion of xenon in water at different temperatures

Niraj Kumar Nepal[1] and Narayan Prasad Adhikari[1]

[1]Central Department of Physics, Tribhuavn University, Kirtipur, Kathmandu, Nepal

Abstract

Molecular Dynamics simulation was performed using 2 xenon atoms as solute and 300 water molecules as solvent. We have studied the structural properties as well as transport property. As structural properties, we have determined the radial distribution function (RDF) of xenon-xenon, xenon-water, and water-water interactions. Study of RDF of xenon-xenon and oxygen-oxygen interactions of water shows that there is hydrophobic behavior of xenon in the presence of water. We have studied the self diffusion coefficient of xenon, water, and mutual diffusion coefficients of xenon in water. The self diffusion coefficient of xenon was estimated using both mean-squared displacement (MSD) and velocity autocorrelation function (VACF), while only MSD was used for water. The temperature dependence of the diffusion coefficient of xenon and water were found to follow the Arrhenius behavior. The activation energies obtained are 12.156 KJ/mole with MSD and 14.617 KJ/mole with VACF in the temperature range taken in this study.

Index Terms: molecular dynamics, xenon, water, diffusion coefficient, hydrophobic interactions

1. Introduction

Water, the most essential component of the nature forms the basic building block of every living and nonliving things, and takes part in almost all natural phenomena. The strong hydrogen bonding between water molecules is responsible for many unusual phenomena where water is a solvent. The noble gases are uncharged and monoatomic particles, and cannot participate in hydrogen bonding. The presence of noble gases in water exhibits a number of uncommon features related to hydration of these gases through the hydrophobic interaction. The transport property such as diffusion of such gases always is of particular interest. We intend to study the different properties of xenon in the presence of water.

Several experimental and theoretical studies have been performed in the past to study the hydrophobic interaction[1] and to estimate the diffusion coefficient of xenon in water.[2-6] However, special consideration is given to the estimation of the diffusion coefficient in this study. There are different methods to estimate the diffusion coefficient. Electron-Spin Resonance (ESR), Dynamic Light Scattering (DLS), and Nuclear Magnetic Resonance (NMR) are some famous techniques which enable us to study the diffusion coefficient.[7] Alternatively, we can estimate the diffusion coefficient by using molecular dynamics (MD) as it provides an opportunity to track the coordinates of all the particles in the system.

MD simulation can be used to study the transport and mechanical properties of complex systems at an atomic level by following the dynamic motion of the particles within the system.[8] Complex systems include biologically operated systems in life, such as the folding of proteins and nucleic acids (adopting specific structures consistent with their function), transportation of ions through membranes, the triggering of series of chemical reactions by enzymes, diffusion of nutrition in hemoglobin, etc.

The organization of the paper is as follows. We present the underlying theory and computational method in Section 2 and Section 3 respectively, while we will discuss our results in Section 4,

and finally, we will conclude the discussion in Section 5.

2. Theory

2.1 Fick's Law and Einstein's Relation

When mass, energy or momentum is transferred through a system, the transport is described to first order by a phenomenological relation of the form,[9]

$$\mathbf{J} = -\text{ coefficient} * \text{gradient} \qquad (1)$$

The flux **J** measures the transfer per unit area in unit time, the gradient provides the driving force for the flux and the coefficient characterizes the resistance to flow. In the case of diffusion, which is the transport of mass, this phenomenological relation leads to Fick's Law,

$$\mathbf{J} = -D\nabla C(r, t) \qquad (2)$$

The vector of the diffusion flux **J** is directed oppositely in direction to the concentration gradient vector ∇C. The concentration gradient vector always points in that direction for which the concentration field undergoes the most rapid increase, and its magnitude equals the maximum rate of concentration at the point. For an isotropic medium the diffusion flux is antiparallel to the concentration gradient. The diffusion flux is expressed in number of particles (or moles) traversing a unit area per unit time and the concentration in number of particles per unit volume. Thus, the diffusivity D has the dimension of length*length per unit time and has the unit [cm^2s^{-1}] or [m^2s^{-1}].[10]

For a diffusing species which obeys a conservation law an equation of continuity can be formulated.

$$\frac{\partial C(r,t)}{\partial t} + \nabla . \boldsymbol{J}(r,t) = 0 \qquad (3)$$

Equation 3 is the continuity equation. Using ***Equation 2*** and ***Equation 3***, one gets[11]

$$D(t) = \frac{1}{6}\frac{\partial}{\partial t} < r^2(t) > \qquad (4)$$

Equation 4 is the famous Einstein relation which relates the diffusion coefficient, a macroscopic transport property of the system, with the mean-squared displacement, a microscopic quantity of the diffusing particles of the system.[11] As in ***Equation 4***, the instantaneous value of the diffusion coefficient can be obtained from the slope of the MSD curve with time. For an MSD that behaves as a straight line after a prolonged period of time, ***Equation 4*** reduces to

$$D = \lim_{t\to\infty} \frac{<r^2(t)>}{6t} \qquad (5)$$

This shows that by tracking the coordinates and hence the position of each particle all the time we can calculate the diffusion coefficient.

2.2. Green-Kubo Formalism (Velocity Auto Correlation Function)

The Green-Kubo formalism relates macroscopic properties (e.g. the diffusion coefficient, in particular a response property of the system) to microscopic properties (fluctuations of the equilibrium distribution). The diffusion coefficient is a response property of the system to a concentration inhomogeneity. The velocity auto-correlation function is an equilibrium property of the system, because it describes the correlations between velocities at different times along an equilibrium trajectory.[11]

$$D = \frac{1}{3}\int_0^\infty d\tau < v_x(\tau)v_x(0) > \qquad (6)$$

The ensemble average term in ***Equation 6*** is the velocity auto-correlation function.

3. Computational Details

The simulation has been carried out using the molecular dynamics simulation package GROMACS 4.6.1 (GROningen MAchine for Chemical Simulation) with GROMOS force field.[13] The system consists of 2 xenon atoms as solute and 300 water molecules as solvent. The first step to start the simulation is to model the system, which is discussed as follows.

3.1 Modeling of xenon and water

Modeling of the system is done by taking the potential energy as a reference. The total potential energy is a combination of different bonded and non-bonded interactions. Bonded interactions include bond stretching, bond-angle vibration, proper dihedral, and improper dihedral. The non-bonded interactions include van der Waals interactions and coulomb interactions. As xenon is a monoatomic noble gas, only contributions from the van der Waals interaction are taken. The non-bonded interactions (van der Waals interactions) between the diffusing particles have been approximated by the Lennard-Jones potential,

$$U_{LJ}(r_{ij}) = 4\epsilon_{ij}[\left(\frac{\sigma_{ij}}{r_{ij}}\right)^{12} - \left(\frac{\sigma_{ij}}{r_{ij}}\right)^{6}] \qquad (7)$$

where, r_{ij} is the distance between two particles *i* and *j*, $2^{(1/6)}\sigma$ is the equilibrium distance between the two particles, and ϵ_{ij} is the strength of the interaction. The GROMACS ***Equation 7*** is modified as,[13]

$$U(r_{ij}) = \frac{C_{12}}{r_{ij}^{12}} - \frac{C_6}{r_{ij}^{6}} \qquad (8)$$

where parameters $C_{12}= 4\epsilon_{ij}\sigma^{12}$ and $C_6= 4\epsilon_{ij}\sigma^{6}$ depends on pair of atom types.

The flexible SPC/E model of water has been used in the present study. It is a semi-empirical model, consisting of three point charges on each atomic site, two in the hydrogen atom and one in the oxygen atom. The values of σ and ε are presented in ***Table 1***. Furthermore, hydrogen and oxygen carry certain charges in a water molecule.

Table 1. L-J Parameters for Xenon[12] and water.[13-15]

Molecule	σ (nm)	ε (K)
Xe	0.39011	227.55 k_B
Water	0.316565	78.197 k_B

Each Hydrogen atom carries a partial charge of +0.4238e, and oxygen atom carries a partial charge of −0.847e where "e" is the elementary charge having magnitude 1.6022×10^{-19}C. In this model the intramolecular potential consists of a harmonic bond and angle vibration terms.

$$U_{OH}(r) = \frac{1}{2}\sum K_{OH}(r - b_{OH})^2 \qquad (9)$$

and

$$U_{OH}(\theta) = \frac{1}{2}K_{HOH}(\theta - \theta_o)^2 \qquad (10)$$

where K_{OH} is the spring constant which measures the strength of the interatomic bond between an oxygen and hydrogen atom; b_{OH} is the equilibrium bond length between oxygen and hydrogen atoms. Similarly, K_{HOH} is the spring constant for bond angle vibration with θ_o as the equilibrium H-O-H bond angle. The parameters that were used for our study are listed in the ***Table 2***. These parameters were presented in the file named spce.itp attached to GROMACS.

Table 2. Intramolecular potential parameters for the flexible SPC/E model of water.[13-15]

Parameters	Values
K_{OH}	$3.45X10^{+05}$ KJ $mol^{-1}\,nm^{12}$
b_{OH}	0.1 nm
K_{HOH}	$3.83X10^{+02}$ KJ $mol^{-1}\,rad^{-2}$
Θ◦	109.47◦

The Lennard-Jones non-bonded parameters for the SPC/E water model are given in ***Table 2***. The parameters for the xenon-water interaction are obtained by using the Lorentz-Bertholet combination rule:

$$\epsilon = \sqrt{\epsilon_{Xe}\epsilon_{water}} \quad ; \quad \sigma = \frac{1}{2}(\sigma_{Xe} + \sigma_{water}).$$

The solution is prepared by using xenon as a solute and water as a solvent with mole fractions of 0.0066 and 0.9934 respectively. The simulation was carried out in a cubic box with dimensions of 2.8 nm shown as in ***Figure 1***. As atoms in water have partial charge, the non-

bonded interaction also includes the Coulomb interaction between the oxygen and hydrogen atoms of two different water molecules, as given by Coulomb's law.

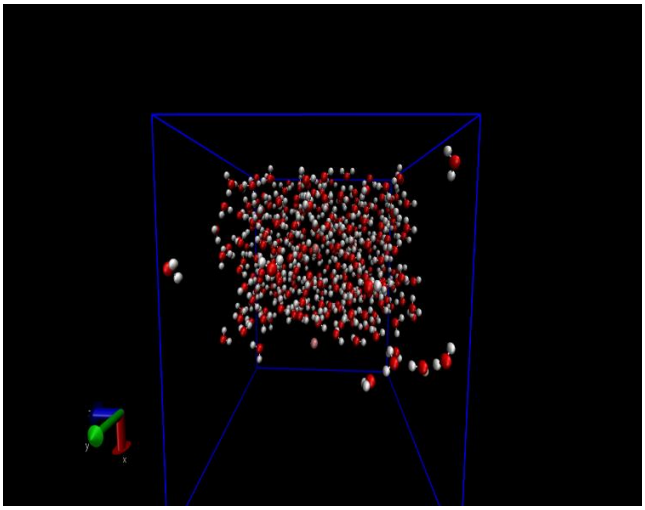

Figure 1. Structure of the system before energy minimization .[16]

3.2 Energy minimization

After solvation, energy minimization is carried out. Energy minimization removes bad contacts between different particles in the system, reduces thermal noise in the structure and brings the system to one of the local minima. The steepest descent algorithm has been used for energy minimization. ***Figure 2*** represents the structure and potential energy versus time plot after energy minimization.

3.3 Equilibration Run

Energy minimization is followed by an equilibration run of 100 ns subjected to NPT ensemble which ensures that the temperature, pressure, and density of the system are fixed at the desired values. This is done to achieve thermodynamic equilibrium, as the dynamic properties like diffusion vary with these parameters. The number of particles within the system is kept fixed by using periodic boundary conditions, where we create replicas of the system (supercell) surrounding the system under study. If a particle leaves the supercell, an exact image enters the supercell from a neighboring replica, keeping the particle number constant. Temperature coupling and pressure coupling are done by velocity-rescale thermostat and Berendsen thermostat respectively. The leap-frog algorithm has been used as an integrator and all bonds are converted to constraints using the SHAKE algorithm. ***Table 3*** lists the temperatures and densities of the system obtained after the equilibration process was carried out for the system structure after energy minimization.

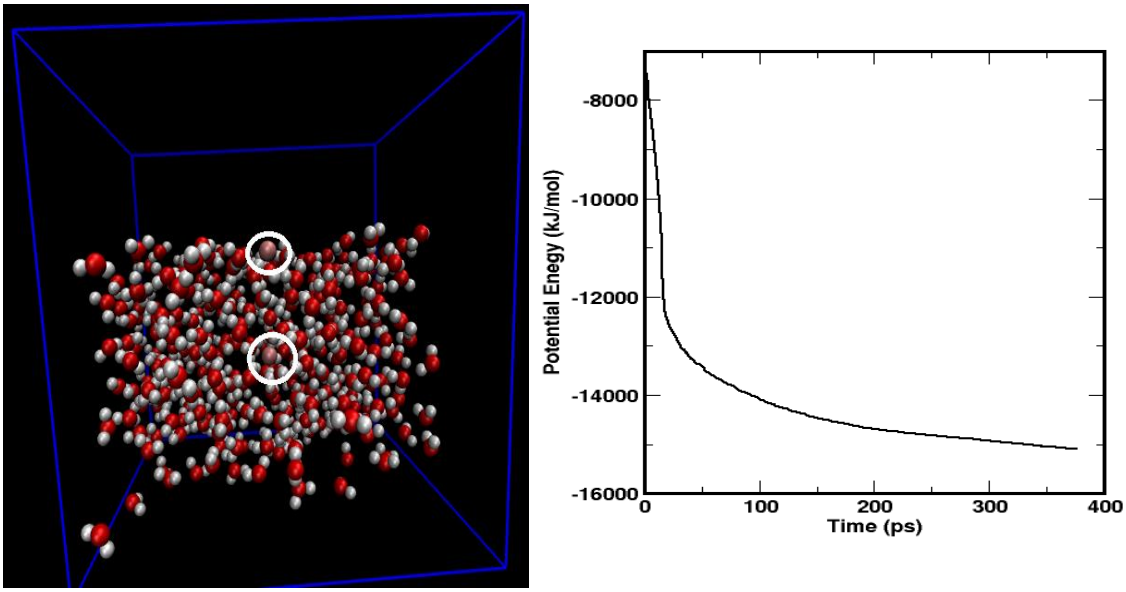

Figure 2. Structure and potential energy of the system after energy minimization. Right panel shows the potential energy as a function of time.

3.4 Production Run

Equilibration is followed by a production run (a final step to calculate the desired dynamic property-diffusion coefficient) where we fix the system volume. So, the system is now an NVT ensemble. A production run is carried out for 200 ns. Pressure coupling is eliminated to ensure it is an NVT ensemble.

Table 3. Values of the simulated temperature (Tsim) and density ρ of the system at various coupling temperatures (T). ρ is the density of the system under study. From ***Table 3***, we see that the density of the system at all the temperatures is found to be close to the density of water, ensuring the validity of the force field parameters we used in the present work.

Temperature (K)	$T_{simulation}$ (K)	Density (Kg/m^3)
303	302.943 ± 0.011	1021.42 ± 0.21
313	312.959 ± 0.013	1015.38 ± 0.14
323	322.952 ± 0.018	1008.51 ± 0.12
333	332.970 ± 0.030	1001.09 ± 0.16

4. Structural Analysis

The structural analysis of the system is performed through the Radial Distribution Function (RDF). In the oxygen-oxygen radial distribution function ($g_{OW–OW}(r)$), OW represents the oxygen atom of the water molecule. The xenon-oxygen radial distribution function ($g_{Xe–OW}(r)$), and xenon-xenon radial distribution function ($g_{Xe–Xe}(r)$) have already been discussed.

4.1 RDF of oxygen-oxygen in water

Figure 3 (left) presents the radial distribution function of oxygen-oxygen in water molecules at different temperatures. The value of $g_{OW–OW}(r)$ is zero up to the certain radial distance from the origin and after that it starts to increase. The region from the origin up to which the value of $g_{OW–OW}(r)$ is zero is called exclusion region. The value of $g_{OW–OW}(r)$ is maximum at a certain radial distance, that point is called the first peak point and corresponding value is the first peak value. The rise and fall in the value of $g_{OW–OW}(r)$ can be seen in ***Figure 3***, giving rise to a second and third peak value. After the third peak, it becomes almost constant. As the peak value decreases and minimum value increases with increasing radial distance and finally becomes constant later. The different peak values with the corresponding points are tabulated in ***Table 4***.

From ***Table 4***, it can be seen that the excluded region of OW-OW interaction lies within 0.247 nm at 303 K, which is less than that of van der Waals radius (0.355 nm) of the oxygen-oxygen interaction. The size of the excluded region seems to be decreasing with increasing temperature. The random motion of the particles increases with an increase in temperature due to thermal agitation. This may increase the probability that the particle comes closer to another particle in spite of its van der Waals interaction range.

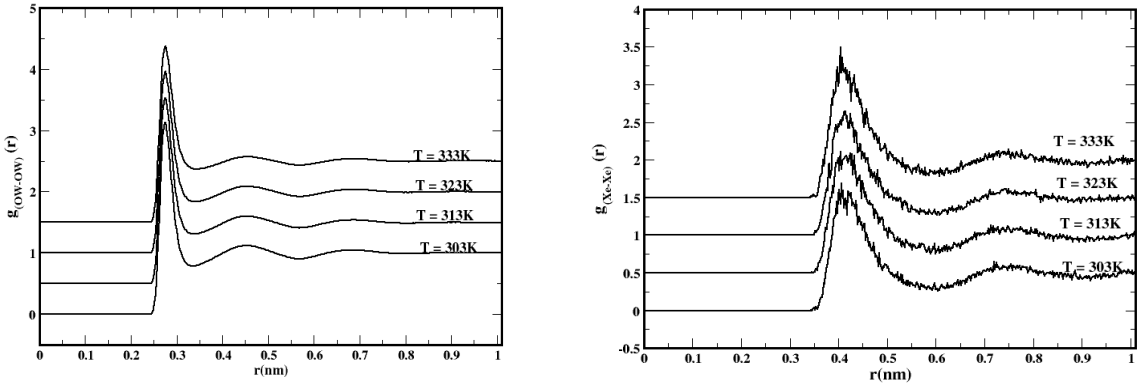

Figure 3. Radial distribution functions, $g_{OW–OW}(r)$ (left) and $g_{Xe–Xe}(r)$ (right) at different temperatures and densities. The RDF at temperatures 313 K, 323 K, and 333 K have been shifted by 0.5, 1.0, and 1.5 respectively along y-axis.

Table 4. RDF, $g_{OW-OW}(r)$, of solvent at different temperatures and different densities. ER: Excluded Region FPP: First Peak Position — FPV: First Peak Value SPP: Second Peak Position — SPV: Second Peak Value TPP: Third Peak Position — TPV: Third Peak Value FMP: First Minimum Position — FMV: First Minimum Value SMP: Second Minimum Position — SMV: Second Minimum Value.

Temperature (K)	ER (nm)	FPP (nm)	FPV	SPP (nm)	SPV	TPP (nm)	TPV	FMP (nm)	FMV	SMP (nm)	SMV
303	0.247	0.276	3.102	0.451	1.104	0.687	1.033	0.340	0.775	0.571	0.902
313	0.246	0.276	3.006	0.453	1.083	0.688	1.027	0.340	0.806	0.571	0.908
323	0.244	0.278	2.933	0.455	1.074	0.688	1.027	0.345	0.827	0.571	0.919
333	0.244	0.278	2.849	0.457	1.058	0.690	1.022	0.346	0.867	0.572	0.931

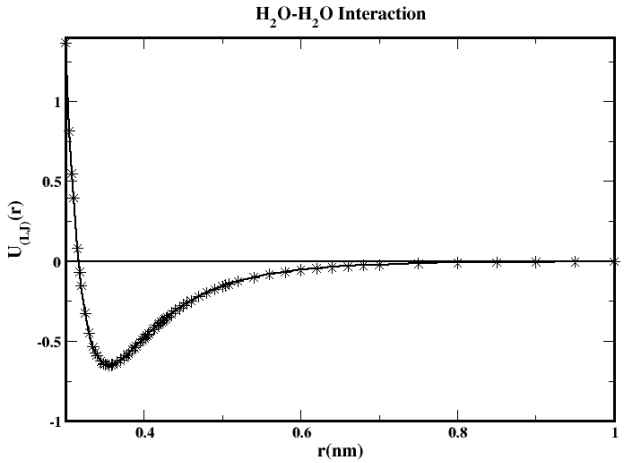

Figure 4. Plot of Lennard-Jones potential as a function of distance for two water molecules.

The first peak values lie within 0.28 nm, which is also less than that of van der Waals radius with a corresponding peak value of about 3.1. This means other potentials along with the Lennard-Jones potential also play a role as seen in ***Figure 4***. In ***Figure 3***, we see that the maximum probability of finding oxygen atoms from other water molecules with respect to a fixed oxygen atom shift left when we consider both the Lennard-Jones and Coulomb potentials acting on the particle compared to when we consider the Lennard-Jones interaction only. Here we consider only two water molecules to get the combined Lennard-Jones and Coulomb potential, as it is difficult to analysis the many body effect on the combined potential. The result we get is consistent with ***Table 4***, where the FPP is less than the van der Waals radius.

Table 4 shows that the peak values decrease with increasing temperature and also the first peak point is shifted to right as the temperature is raised. It can also be seen that the first minimum point increases and the exclusion region decreases with increasing temperature. This will increase the width of the peak as the temperature is raised. The decrease in height and increase in width of the first peak of $g(_{OW-OW}(r))$ point to a change in the nearest neighbor coordination number[1] which indicates that the solvent becomes less structured as the temperature increases. Similarly, the second and third peak points and corresponding values show similar results to that of first peak.

4.2 RDF of xenon-xenon interaction

Figure 3 (right) is the radial distribution function of xenon $g(_{Xe-Xe}(r))$ at different temperatures. Also the Van der Waals radius of xenon is 0.438 nm for the system under study. As is seen from ***Figure 3*** (right), the excluded regions for xenon atoms lie within 0.345 nm, where $g(_{Xe-Xe}(r))$ is zero, as it is less than the van der Waals radius of

xenon. There are no atoms present within this region.

The roughness in the figure is due to insufficient statistics caused by the small number of xenon atoms. The first peak occurs around 0.42 nm, where the probability of finding xenon atoms is a maximum. The distance at which the first peak occurs is called nearest neighbor separation, which is less than the van der Waals radius, which may be due to the tendency of noble gas to aggregate in the presence of water. The second peak occurs at around 0.76 nm. Further the presence of the first and second peaks signifies that the xenon atoms do not move independently but are correlated to some extent though small in number.

As can be seen from ***Figure 3*** (right), the gap between two successive peaks is increasing with increase in temperature. This is opposite to the case of the oxygen-oxygen interaction within water, where these peak values decrease with increasing temperature. This means that the xenon atoms tend to aggregate with increasing temperature. However, the oxygen atoms of the water molecules move away from each other with increasing temperature. The unusual thermo-physical properties of dilute solutions of nonpolar substances in water are usually explained as "hydrophobic interactions" - special interactions between two or more nonpolar solute molecules in water, solute interactions with water molecules, and interactions between water molecules in the vicinity of these solutes.

4.3 RDF of xenon-oxygen interaction

The radial distribution function of solvent with respect to xenon atoms, $g_{Xe-OW}(r)$, in the system at different temperatures and corresponding system densities have been studied. The plot of RDF at different temperatures is shown in ***Figure 5***. The excluded regions remain confined within 0.305 nm, which is less than the Van der Waals radius 0.397 nm of the xenon-water interaction. The position of the first peaks is fixed at around 0.381 nm. The first peak value decreases with a rise in temperature by small amounts for the first parameter and also for the second parameter except at 323 K. The second peaks also seem to be fixed at 0.666 nm. Moreover, the widths of the peaks increase with the increase in temperature. This signifies that the correlation between the xenon and solvent molecules decreases as temperature is increased, which is due to the thermal energy acquired by them as it is proportional to temperature. ***Table 5*** gives the details of the radial distribution function of the solvent molecules with respect to the xenon atoms.

Table 5. RDF, gXe−OW(r), of solute-solvent at different temperatures and different densities.

Temperature (K)	ER (nm)	FPP (nm)	FPV	SPP (nm)	SPV	FMP (nm)	FMV	SMP (nm)	SMV
303	0.306	0.381	1.951	0.666	1.093	0.555	0.744	0.926	0.979
313	0.307	0.381	1.901	0.666	1.073	0.555	0.758	0.926	0.979
323	0.305	0.381	1.878	0.666	1.069	0.555	0.768	0.926	0.982
333	0.305	0.381	1.871	0.668	1.073	0.555	0.772	0.926	0.986

4.4 Self-Diffusion Coefficient

The self diffusion coefficient is obtained through the Mean Square Displacement (MSD) method and the Velocity autocorrelation (VACF) method. ***Figure 6*** presents the plot of the MSD vs time at different temperatures. Although the production run for the NVT ensemble is 200 ns, we have truncated the MSD versus time graph to 2 ns for better statistics. The slope of this graph divided by 6 gives the self-diffusion coefficient. The graph shows that the MSD varies linearly with time as expected. The MSD increases with the temperature, indicating that the diffusion coefficient increases with increasing temperature. This is because with an increase in temperature the density of system decreases, thereby increasing the space available for xenon atoms to execute a random walk. The self diffusion

coefficient is estimated after the system attains the equilibrium state, i.e. has zero concentration gradient, which can be illustrated by using a logarithmic plot of the MSD vs time and a plot of the diffusion coefficient vs time.

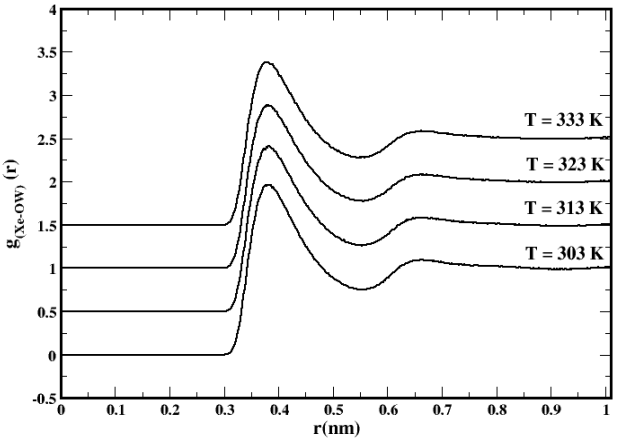

Figure 5. Radial distribution function, $g_{Xe-OW}(r)$, at different temperatures and corresponding densities. The RDF at temperatures 313 K, 323 K, and 333 K have been shifted by 0.5, 1.0, and 1.5 respectively along y-axis.

In the logarithmic plot of the MSD vs time, it can be seen that the MSD follows a parabolic profile, which can be explained by using the diffusion coefficient vs time plot. This shows that diffusion coefficient is high at first which is due to the ballistic motion of xenon atoms, then, after a certain time, the graph is almost constant, showing that the system is in an equilibrium state. ***Figure 7*** shows the variation of the velocity-autocorrelation function with time at 303K. The values of the diffusion coefficient of xenon obtained by using the two approaches, namely the MSD and VACF, at different temperatures is tabulated in ***Table 6***. The self diffusion coefficient increases with an increase in temperature, as expected. This is because of the increase in velocity of the xenon atoms in accordance with the increase in temperature. Also, the density of the system decreases and the space available for the xenon atoms to execute random walk motion increases. Similarly, the self diffusion of water has been discussed. The value of the self diffusion coefficient of water with respect to xenon has been compared to the experimental value of the self diffusion coefficient of pure water. The value obtained in the present work is slightly less than that of pure water which may be accounted by the hydrophobic interaction between the noble gases and water.

4.5 Diffusion Coefficient as a function of temperature

In the previous section, we saw that the diffusion coefficient increases with increasing temperature. However, we didn't discuss the exact behavior of the dependence of the diffusion coefficient with temperature. In this section, we discuss that behavior. Like chemical reactions, diffusion is also a thermally activated process, as the kinetic energy of atoms and molecules increases with increase in temperature. This ultimately increases the velocity of the particles which governs the change in diffusion rate. The temperature dependence of diffusion appears in the form of an Arrhenius-type equation[11]

$$D = D_o \exp(-\frac{E_a N_A}{k_B T}) \qquad (12)$$

where D_o is the pre-exponential factor, N_A is the Avogadro number having value of $6.022X10^{23}$ per mole, and k_B is the Boltzmann constant having value equal to $1.38X10^{-23}$ J/K. E_a is the activation energy.

Rewriting ***Equation 12*** we get

$$\ln\left(\frac{D}{D_o}\right) = -\frac{E_a N_A}{k_B T} \qquad (13)$$

Thus a plot of ln(D) against 1/T should be a straight line if the diffusion coefficient follows Arrhenius behavior. ***Figure 9*** shows that Arrhenius behavior is followed by the diffusion coefficient. The experimental fit is obtained using values available in the literature.[2] The activation energy of xenon is 12.156 KJ/mole with MSD and 14.617 KJ/mole with VACF. The value of the activation energy is quite close to the experimental value of 12.8 KJ/mole.[3] Also the activation energy of the SPC/E water model has been estimated. The activation energy of water obtained with MSD in the present work is 14.69

KJ/mole, which is close to the experimental value of 16.927 KJ/mole.[17]

5. Conclusions

The diffusion coefficients obtained are quite close to the values reported by Jahne *et al.*[5] at 303 K and Weingartener *et al.*[3] at 323 K. The value of the activation energies obtained with these parameters, 12.156 KJ/mole with MSD and 14.617 KJ/mole with VACF, are quite close to 12.8 KJ/mole obtained with the 129Xe NMR method.[3] The hydrophobic nature of xenon in the presence of water is confirmed via RDF analysis of xenon-xenon and oxygen-oxygen interaction.

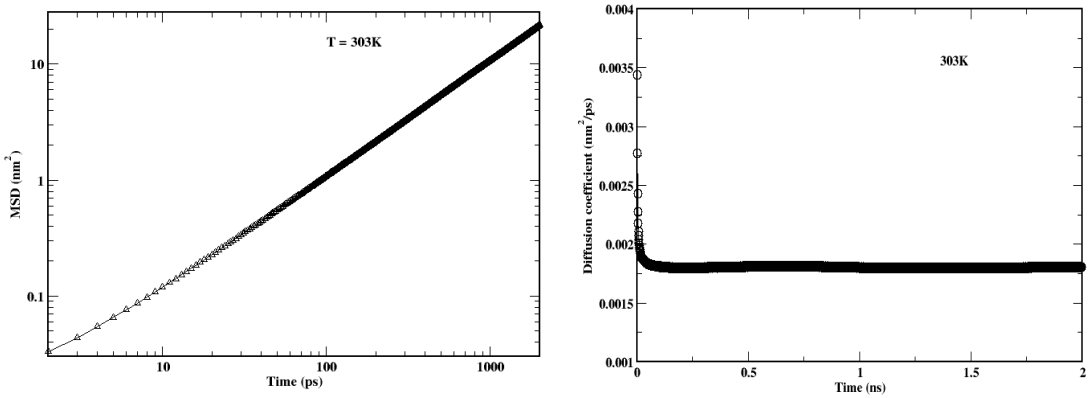

Figure 6. Logarithm plot of MSD vs time for xenon as a function of time at temperature 303 K in left and the plot of self-diffusion coefficient vs time in right at same temperature.

Acknowledgements

NKN thanks Dipendra Bhandari, Keshav Sharma Paudel, and Ishwar Poudel for fruitful discussions.

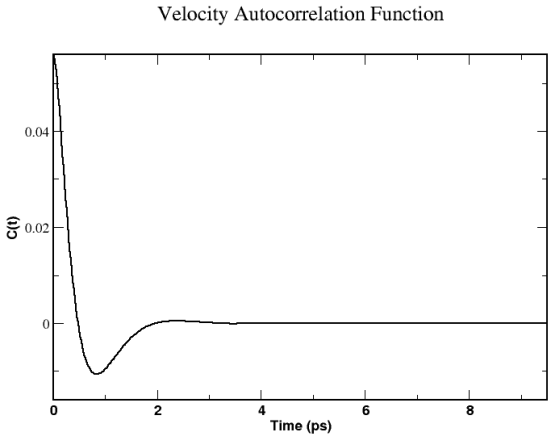

Figure 7. Variation of velocity auto-correlation function for xenon as a function of time at T=303K.

Table 6. Experimental and simulated values of the self-diffusion coefficient of Xe and the SPC/E model of water at different temperatures. D_{Xe} is the self-diffusion coefficient of xenon in water and D_{water} is that of water.

	D_{Xe} ($\times 10^{-9} m^2 s^{-1}$)			D_{water} ($\times 10^{-9} m^2 s^{-1}$)	
Temperature (K)	Experimental	Simulated		Experimental [17]	Simulated (MSD)
303	1.08 [2], 1.70 [5]	1.80	1.99	2.59	2.51
313	1.56 [2]	2.35	2.23	3.24	3.10
323	2.27[2],2.81[3]	2.61	2.89	3.97	3.65
333	3.98[2]	2.83	3.28	4.77	4.28

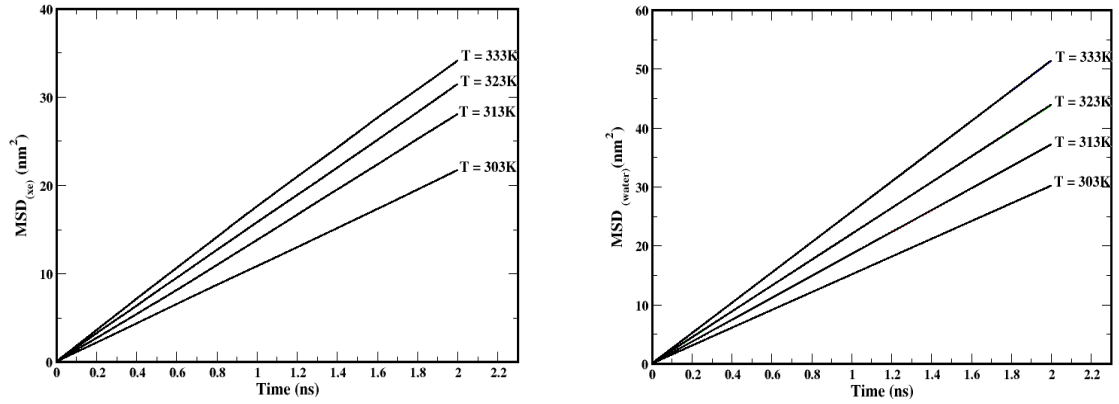

Figure 8. The MSD of xenon and water as a function of time at temperatures 303 K, 313 K, 323 K, and 333 K. The plot for xenon is on the left and that of water on the right.

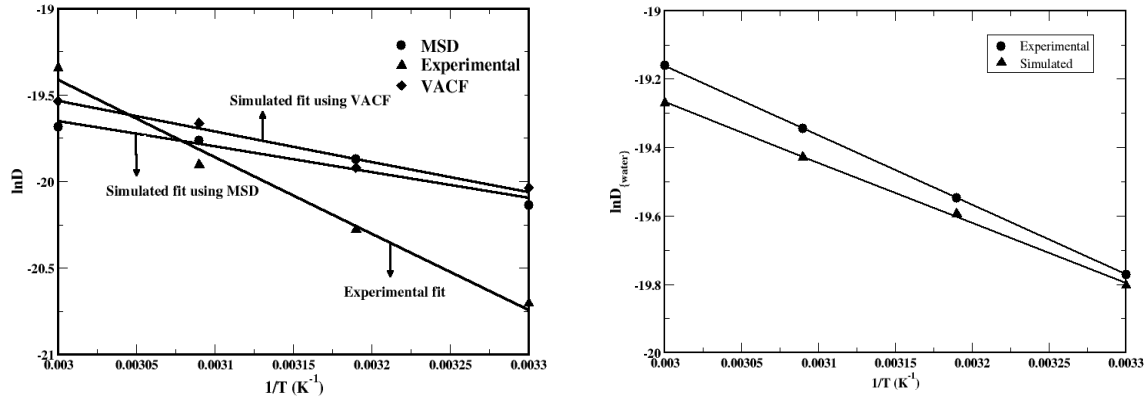

Figure 9. Comparison of an Arrhenius plot of the self-diffusion coefficients of Xe (left) and of water (right) with experimental fits. The experimental fits of xenon[2] and water[17] have been obtained by plotting values available in the literature.

References

[1] O. Coskuner and U. K. Deiters, *Z. Phys. Chem*., **2007**, 221, 785.

[2] D. L. Wise and G. Houghton, *Chem. Eng. Sci.*, **1968**, 23, 1211.

[3] H. Weingartner, R. Haselmeier and M. Holz, *Chem. Phys. Lett*., **1992**, 195 (5), 596.

[4] A. J. H. Boerboom and G. Klein, *J. Chem. Phys*., **1969** 50, 1086.

[5] Jahne, B., Heinz, G., and Dietrich, W., *J. Geophys. Res*., **1987**, 92, 10767.

[6] J. Wolber, S. J. Doran, M. O. Leach and A. Bifone, *Chem. Phys. Lett*., **1998**, 296, 391.

[7] P. Heitjans and J. Krager, Diffusion in Condensed Matter: Methods, Materials, Models, **2009**, Springer, New York.

[8] J. Meller, Molecular Dynamics, **2001**, John Wiley & Sons, New York.

[9] J. Crank, The Mathematics of Diffusion, 2nd ed., **1975**, Oxford University Press, Oxford.

[10] H. Mehrer, Diffusion in Solids; Fundamentals, Methods, Materials, Diffusion-Controlled Processes, **2007**, Springer Series in Solid State Science, 155, Berlin.

[11] D. Frankel, B. Smit, Understanding Molecular Simulation From Algorithms to Applications, **2002**, Academic Press, USA.

[12] J.Vrabec, J. Stoll and H.Hasse, *J. Phys. Chem. B*, **2001**, 105, 12126.

[13] D. van der Spoel, E. Lindahl, B. Hess, A. R. van Buuren, E. Apol, P. J. Meulenhoff, D. P. Tieleman, A. L. T. M. Sijbers, K. A. Feenstra, R. van Drunen and H. J. C.

Berendsen, Gromacs User Manual version 4.5, **2010**, www.gromacs.org.
[14] H. J. C. Berendsen, J. R. Grigera and T. P. Straatsma, *J. Phys. Chem*., **1987**, 91, 6269.
[15] P. Mark and L. Nilson, *J. Phys. Chem. A*, **2001**, 105, 9954.
[16] W. Humphrey, A. Dalke, and K. Schulten, *J. Molec. Graphics*, **1996**, 14, 33.
[17] A. J. Eastel, W. E. Price and L. A. Woolf, *J. Chem. Soc., Faraday Trans. 1*, **1989**, 15, 1091.

Effect of fragmentation of kerangas forest on small mammal community structure in Brunei Darussalam

Siti Salwa Abd Khalid[1] and T. Ulmar Grafe[1,2]*

[1]Institute for Biodiversity and Environmental Research, Universiti Brunei Darussalam, Jalan Tungku Link, Gadong, BE 1410, Brunei Darussalam
[2]Faculty of Science, Universiti Brunei Darussalam, Jalan Tungku Link, Gadong, BE 1410, Brunei Darussalam

**corresponding author email: salwa.khalid@ubd.edu.bn*

Abstract

Widespread and rapid forest loss and disturbance have resulted in increased fragmentation of tropical forests. The impacts of forest disturbance and fragmentation on small mammals have been widely studied across the tropics and these studies have highlighted the detrimental effects. However, there is limited understanding on the impacts on small mammals in Borneo. This study investigated the impacts of fragmentation on small mammal community structure in lowland coastal heath forests known as kerangas forests, in Brunei Darussalam. Twelve study sites were compared in three forest types: fragmented (2.07-17.6 ha), disturbed (443.55-483.79 ha) and undisturbed (>500 ha) forests. In addition, the correlations between species richness, abundance and biomass of small mammals, and forest size were investigated. There was a clear change in species composition in the different forest types. Fragmented forests had the lowest species richness but the highest pooled abundance and biomass compared with disturbed and undisturbed forests. Species richness increased with forest size as predicted by the theory of island biogeography. In contrast, abundance and biomass was negatively correlated to forest size. Factors that contribute to the pronounced decline in species richness in fragmented forests include loss of rare and native forest species, reduced forest size in fragmented forests and distance effect. We suggest that a release from top-down control by predators and favourable conditions as a result from forest fragmentation are responsible for higher abundance and biomass of small mammals in fragmented forests.

Index Terms: deforestation, extinction, landscape ecology, rodents, tropical rain forest

1. Introduction.

Forest disturbance including forest fragmentation is recognized as one of the major threats to biodiversity.[1-3] Forest fragmentation is of great concern especially in the tropics because tropical forests are among the most biodiverse places remaining on earth but also where the deforestation rate is highest.[4,5] Forests in Borneo in particular are continuing to decline at an accelerating rate, becoming increasingly fragmented and in many areas only small forest patches remain.[6] Small mammal communities show diverse responses to forest fragmentation, including changes in species richness and abundance,[7,8] loss or decline of species with specific requirements,[9,10] species invasions,[10] changes in community trophic structure,[10] and changes in movement patterns.[11]

The Island Biogeography theory[12] proposed that the number of species found in an island was determined by immigration and extinction. Immigration and extinction, in turn are influenced by distance and area. The two main predictions of island biogeography theory are that: (1) islands close to a source area should have a higher number of species than islands further from the source area; and (2) for islands

located at similar distance from the source area, larger islands should have more species than smaller islands.[12] This theory can be adapted to habitat islands such as fragmented forests.

Forest fragmentation has been characterized by reduced patch size and increased patch isolation, each of which has distinctive impacts on biodiversity. The effects of forest fragmentation on small mammals have been widely studied in the tropics (e.g., Amazon,[7,9,13] Australia,[14] Madagascar,[15] Thailand[16]). Some studies found positive effects such as higher species richness, abundance and biomass of small mammals in fragmented forests compared with continuous forests.[7,13] Others reported negative results such as a decline in species richness and abundance with decreasing fragment size[14,15] and extinction of certain species.[9,16] Given that these studies have mostly highlighted the detrimental effects of forest fragmentation, we should expect a similar reduction in species richness and abundance of small mammals in fragmented forests on Borneo.
Studies on the effects of forest fragmentation in Borneo are limited. Previous studies on faunal communities were based mostly on butterflies,[17-19] ants,[20,21] spiders,[22] frogs,[21] and birds.[23,24] Only a few studies looked at the effects of fragmentation on small mammals in Borneo.[8,10,11,25-27] Moreover, most studies on small mammals in Borneo have concentrated on the effects of logging in dipterocarp forests.[25,28-36] Some have found that logging has negative consequences on species richness and abundance. For example, species richness and abundance were lower in logged forests compared with primary forests.[29,31] Others have noted the opposite results, with increased species richness and abundance in logged forests compared with unlogged forests.[34,35] The disparity in their results might be because of small sampling areas and unequal number of samples,[34] but clearly more knowledge is needed on the impact of forest disturbance including fragmentation on small mammal communities including kerangas forests.

Kerangas or heath forest is characterized by its low uniform canopy (10m height compared to dipterocarp forest which is usually 40-60m in height) with no emergent trees and dense stands of small pole-sized trees that develop on acidic sandy soils that are nutrient deficient.[37] Kerangas forests are rare and occupy only 1.46 percent (6 558 ha) of Brunei Darussalam's land mass.[38] Kerangas forests are found mainly in the coastal area where most of the residential and infrastructure development occurs; as such, many are now fragmented patches. Only 23 percent of pristine kerangas forests remain.[38] Furthermore, kerangas forests are continuing to decline because of increased development as well as recurring disturbances such as fire and invasion by exotic tree species (*Acacia* spp.).[39] Kerangas forests generally have less biodiverse faunal communities compared with dipterocarp forests on Borneo (e.g., birds[40]).

Small mammals play an important ecological role. They are important prey items for a number of predators such as barn owls, *Tyto alba javanica*[41] and leopard cats, *Prionailurus bengalensis bornensis.*[42] In addition, they are important seed predators and dispersers of many tree species contributing to forest regeneration and the maintenance of diversity of tropical forests.[43-46] Loss or defaunation of small mammals in forest ecosystems can impact the important small mammal-dependent ecological processes which can have a major effect on the stability and/or resilience of forests. For example, reductions in rodent functional diversity have caused a decline in the abundance of small-seeded plant species.[49] Therefore, faunal studies in this type of forest is of considerable ecological interest.

In this study, the impacts of forest disturbance, including forest fragmentation on the species richness and faunal composition of small mammals in kerangas forest in Brunei, were examined. Specifically, the aims of the study were to answer the following questions: (1) what small mammals are found in the fragmented, disturbed and undisturbed kerangas forests? Is there any difference in the small mammal species composition between the different forest types? (2) Does the species richness, abundance and biomass of small mammals differ in fragmented, disturbed and undisturbed kerangas forests? (3) Do the species richness, abundance and biomass of small mammals differ in different sized forest?

2. Experimental.

2.1 Study site

The study was conducted in twelve study sites in Brunei Darussalam: four in fragmented forests, four in disturbed forests and four in undisturbed forests (see **Figure 1**). All study sites were between 0.28 and 48.77 km (mean 26.13 ± 22.8) apart. The four fragmented forest study sites were located in the Brunei-Muara district, specifically in Kampong Rimba (N 4˚.4", E 114˚54'29.6"). The conversion of continuous kerangas forest into isolated forest patches occurs mainly in this area due to housing developments. They were isolated and separated from each other by drains, roads, houses, and the matrix. The fragmented forests were F1 (2.07 ha), F2 (17.6 ha), F3 (4.47 ha) and F4 (17.13 ha).

Disturbed forests refer to areas that have had anthropogenic disturbance such as fire or logging that have led to noticeable changes in terms of forest composition and structure. Two disturbed forest study sites were located in Brunei-Muara district (N 4˚58'58.8", E 114˚54'34.1"). D1 and D2 (both 443.55 ha) were located in disturbed kerangas forest that had been subjected to repeated forest fires and were extensively covered by the invasive species, *Acacia mangium* and *A. auriculiformis*. D1 and D2 were located 2.24 km apart and were separated by a trail (3 m in width) that was established for an underground gas pipeline. D2 was affected by forest fires in

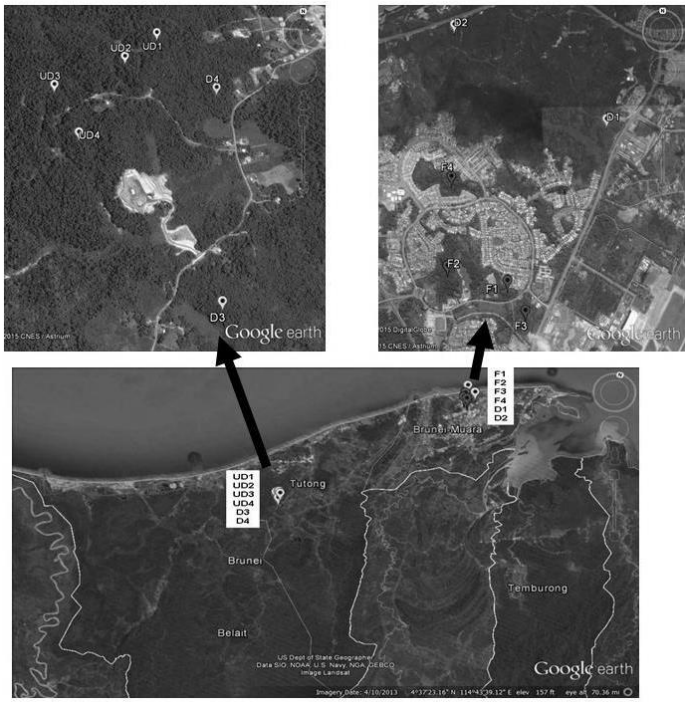

Figure 1. The study area in Brunei Darussalam and locations of the twelve study sites.

February 2013, during the field study period and thus, D1 and D2 were not structurally similar. D2 had disrupted canopy, pronounced gaps (canopy cover of 43.16 ± 21.37 %) and thick undergrowth covered with *Imperata cylindrica* (lalang grasses) and *Dicranopteris* spp. D1, in contrast, had canopy cover (85.44 ± 5.81 %) and less thick undergrowth. The other two disturbed forest study sites (D3 – 483.79 ha and D4 >500 ha) were located in the Tutong district (N 4˚38'55.6", E 114˚37'36.7"). D3 and D4 were old secondary kerangas forests which were clear felled 40–50 yrs prior to this study. D3 and D4 had understory that was typically covered by dense vegetation of abundant plant species, such as ginger (Zingiberaceae) and rattan *Calamus* spp., and *Hevea brasiliensis* (rubber tree). Undisturbed forests refer to primary forest areas that are relatively undisturbed by anthropogenic influences that could cause changes in forest structure. However, poaching and hunting do occur in these forests so there is some degree of anthropogenic disturbance. The four undisturbed forest study sites were located in a continuous pristine forest of the Andulau Forest Reserve (N 4˚39'38.4", E 114˚37'24.1") in Bang Nalud in the

Tutong district. All these undisturbed forest study sites comprised more than 500 hectares. UD1 was dominated by the endemic and endangered conifer *Agathis borneensis* (tulong).

2.2 Trapping protocol

Small mammals were captured with collapsible cage traps (30 cm long x 14 cm wide x 14 cm high)[9] between May 2012 and March 2014. The targeted small mammals were non-volant mammals (thus excluding bats) including tree shrews (Tupaiidae), rats (Muridae) and squirrels (Sciuridae). An index lines technique was employed at each study site where a 200-m line transect was established with 63 cage traps in total set along the transect at 10-m intervals.[48] At each trapping point, one above-ground trap between 18 and 176 cm above ground height (mean 82.52 ± 33.31) and two traps on the ground were set with the location of traps remaining constant throughout the sampling period. We conducted 36 trapping sessions, alternating between the twelve study sites with a mean interval of 20 ± 16 d between sessions along the same transect line, giving a total of three sampling units per site. Trapping was carried out for 7 consecutive days and nights during each trapping session. The traps were baited with aromatic banana (pisang rasthali) which has been shown to be the most effective bait for attracting small mammals.[8,10] Because bananas were the only baits used for this study, the targeted species were limited to omnivores and frugivores. Baits were replaced every evening (only once per day) throughout the trapping session. The traps were checked for animals every morning and evening. Animals that were trapped both in the morning and evening of the same day account for the previous trap night. The trapping effort was 441 trap nights (traps active for 24 h) per session, giving a total of 15 876 trap nights. Captured animals were marked with non-toxic dyes (Artline, Shachihata), sexed and then released at the point of capture. The dyes were reapplied during capture, which lasted throughout the trapping sessions. Species identification was based on Phillipps and Phillipps.[49] All animal handlings were approved by the University Research Ethics Committee (UREC), Universiti Brunei Darussalam, and followed the guidelines given by the American Society of Mammalogists.[50]

2.3 Data analysis

The relative abundance of small mammals at each study site was calculated as the number of individuals trapped per 100 station nights. This index provides a more accurate indicator of relative abundance than trap nights.[51] Relative biomass was calculated as the total weight of all individuals trapped per 100 station nights.[51,52] Species richness was calculated as the total number of species captured during the trapping session. Non-parametric estimators (Chao2 and Jackknife1) were also used to estimate the true number of species expected to be present in each study site.[53] Three Chao and Jackknife replications were used. Chao and Jackknife estimators are effective and provide accurate predictions of species richness from small samples.[54,55] The Species Diversity and Richness 2.65 program[56] was used to estimate species richness. The non-parametric Kruskal-Wallis (K-W) test was used to compare species richness between study sites and forest types. The total number of species, relative abundance and relative biomass were correlated with forest size using Pearson correlation test. The total number of species were log 10 transformed for achieving normality. Statistical analyses were performed with SPSS 20.0.[57] Means are given as $\bar{X} \pm 1\ SD$. Cluster analysis was performed using the PC-ORD version 6 program.[58] Sorensen distance measures was used based on group average to define small mammal community correlations among sites and produce a dendrogram.

3. Results and Discussion.

A total of 353 individuals were captured (2849 times trapped) from 13 species, representing eight genera from four families (see ***Table 1***). In the fragmented forests (F1-F4), only three species but more individuals (183 individuals) were recorded compared with disturbed and undisturbed forests. In the disturbed forests D1 and D2 in Brunei-Muara, there were fewer species but more individuals (4 species, 60 individuals) recorded than in the disturbed forests

D3 and D4 in Tutong (9 species, 27 individuals). In the undisturbed forests, more species but fewer individuals (8 species, 83 individuals) were recorded. The disturbed forest D4 had the highest number of species captured (eight species) but contained the lowest number of individuals (nine individuals) among all study sites.

Callosciurus notatus (plantain squirrel) was the only species captured in all 12 study sites (see ***Table 1***). *Sundamys muelleri* (Müller's rat) was captured in all fragmented forests and the two disturbed forests D1 and D2 in Brunei-Muara, but not in the disturbed forests in Tutong (D3 and D4) or in any undisturbed forests (see ***Table 1***). *Sundamys muelleri* was the dominant species (*i.e.* with highest number of individuals captured compared with other species) present in all fragmented forests and two disturbed forests D1 and D2 in Brunei-Muara (see ***Table 1***). *Tupaia minor* (lesser tree shrew) was another species that was commonly found in disturbed habitats.[8,10] It was captured in all fragmented forests and disturbed forest D2, but not in disturbed forests D1, D3 and D4 or in undisturbed forests (see ***Table 1***).

Table 1. Mean number of individuals (averaged over three replicated capture sessions) for all species trapped in the study sites. The total times trapped for all study sites are in parenthesis.

	Fragmented forests				Disturbed forests				Undisturbed forests			
Species	F1 (563)	F2 (390)	F3 (321)	F4 (413)	D1 (170)	D2 (270)	D3 (163)	D4 (53)	UD1 (52)	UD2 (165)	UD3 (149)	UD4 (140)
Sundamys muelleri	21	16	11	22	8	14	-	-	-	-	-	-
Maxomys rajah	-	-	-	-	-	-	2	5	3	4	4	2
Maxomys whiteheadi	-	-	-	-	-	-	1	-	-	-	-	-
Leopoldamys sabanus	-	-	-	-	-	-	-	1	1	-	-	-
Niviventer cremoriventer	-	-	-	-	-	-	3	2	-	-	-	-
Callosciurus notatus	19	8	11	6	3	6	1	0.33	1	3	1	6
Sundasciurus hippurus	-	-	-	-	-	-	-	-	-	0.33	-	-
Tupaia minor	12	10	7	3	-	9	-	-	-	-	-	-
Tupaia picta	-	-	-	-	4	2	-	2	3	5	9	3
Tupaia tana	-	-	-	-	-	-	-	2	-	2	3	4
Tupaia longipes	-	-	-	-	-	-	-	1	-	-	-	0.33
Tupaia gracilis	-	-	-	-	-	-	-	0.33	0.33	-	-	-
Echinosorex gymnura	-	-	-	-	-	-	-	-	1	-	-	0.33
Number of species	3	3	3	3	3	4	4	8	6	5	4	6

Tupaia picta (painted tree shrew) was captured in disturbed forests (except D3) and undisturbed forests but not in fragmented forests (see ***Table 1***). *Maxomys rajah* (brown spiny rat) was captured in all study sites in Tutong, including the two disturbed forests (D3 and D4) and undisturbed forests, but not in the study sites in Brunei-Muara (see ***Table 1***). *Sundasciurus hippurus* (horse-tailed squirrel), listed by the IUCN as near threatened,[60] was captured only once in the undisturbed forest plot UD2. This species is rare and increasingly difficult to find because it has a large home range and is nomadic within that home range.[49]

The mean relative abundance and biomass were much higher in fragmented forests than in disturbed and undisturbed forests (K-W, $P < 0.05$, see ***Table 2***). Site F1, the smallest fragmented forest (2.07 ha) had the highest relative abundance and total biomass (see ***Table 2***). Site D3, one of the disturbed sites in Tutong, had the lowest relative abundance and biomass (see ***Table 2***).

The study sites were clustered into two main groups based on the small mammal species composition (see ***Figure 2***). The first group contained all four fragmented forests and two disturbed forests (D1 and D2 in Brunei-Muara).

The second group contained all four undisturbed forests and two disturbed forests (D3 and D4 in Tutong) (see ***Figure 2***). Based on cluster analysis, there were two cluster dominated by different species: (1) *S. muelleri, C. notatus* and *T. minor;* and (2) *M. rajah, M. whiteheadi, L. sabanus, N. cremoriventer, S. hippurus, T. picta, T. tana, T. longipes, T. gracilis* and *E. gymnura*.

Table 2. Mean relative abundance (mean number of individuals trapped per 100 station nights) and mean relative biomass (total weight (g) of all individuals trapped per 100 station nights). Means are given as $\bar{X} \pm 1$ SD.

Study Site	Relative Abundance	Relative Biomass (g)
Fragmented forests	**8.24 ± 2.66**	**1440 ± 402**
F1	11.94 ± 2.5	1898 ± 544
F2	7.71 ± 1.71	1376 ± 240
F3	6.42 ± 0.35	1128 ±125
F4	6.88 ± 1.02	1359 ± 201
Disturbed forests	**3.91 ± 2.20**	**580 ± 316**
D1	3.25 ± 0.47	655 ± 94
D2	7.03 ± 1.18	933 ± 206
D3	1.36 ± 0	161 ± 68
D4	4 ± 0.13	573 ± 188
Undisturbed forests	**3.06 ± 1.22**	**533 ± 201**
UD1	1.96 ± 1.05	443 ± 218
UD2	3.18 ± 1.04	593 ±147
UD3	3.71 ± 1.25	501 ± 196
UD4	3.4 ± 1.38	675 ±259

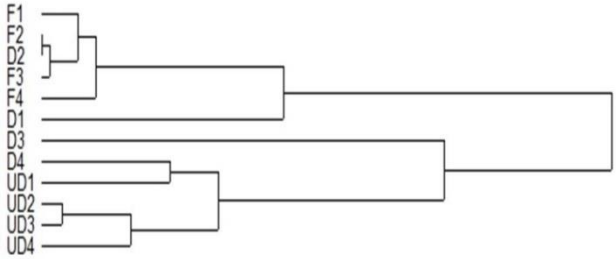

Figure 2. Dendrogram showing the similarity between small mammal species community in all study sites.

Species richness was significantly different between sites (see ***Figure 3***): observed species richness (K-W, $P = 0.004$), Chao2 (K-W, $P = 0.001$) and Jackknife (K-W, $P = 0.002$).

The number of species trapped was positively correlated with forest size (Spearman's $r = 0.730$, $P < 0.0001$, see ***Figure 4A***). In contrast, the relative abundance and biomass were negatively correlated with forest size (Pearson's $r = -0.502$, $P = 0.001$ and $r = -0.514$, $P = 0.001$ respectively, see ***Figure 4B*** and ***C***).

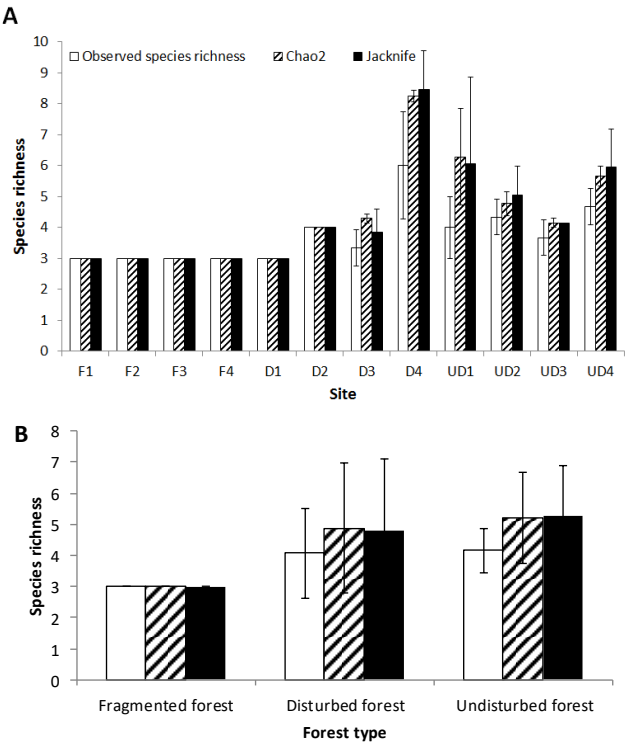

Figure 3. Species richness of small mammals (Mean ± 1 SD) for (**A**) all study sites, and (**B**) all forest types. Clear columns refers to the number of species captured during the trapping sessions, striped columns refers to the estimated number of species based on Chao2 estimates, and black columns refer to Jackknife estimates.

The species richness, abundance and biomass of small mammals in kerangas forests were found to be affected by forest disturbance including fragmentation. Fragmented forests had the lowest species richness compared with disturbed and undisturbed forests. A total of ten species were not recorded in fragmented forests. Only three small mammal species were recorded in all the fragmented forests: Müller's rat, lesser tree shrew, and plantain squirrel. These species are commonly found in disturbed habitats[10] and are of low conservation concern.[60] The presence of these three species in all the fragmented forests suggests that they are tolerant of forest fragmentation. Similar results of low species richness in fragmented forests were obtained in the tropical forests of the Amazon basin.[61] This study also demonstrates a strong correlation between forest size and species richness of small

mammals in kerangas forest. Species richness increased with forest size as predicted by the island biogeography theory.[12] However, forest size is not independent of the different forest types and hence, it's difficult to distinguish between the effects of forest size and forest types as a possible driver of gradients in species richness, abundance and biomass.

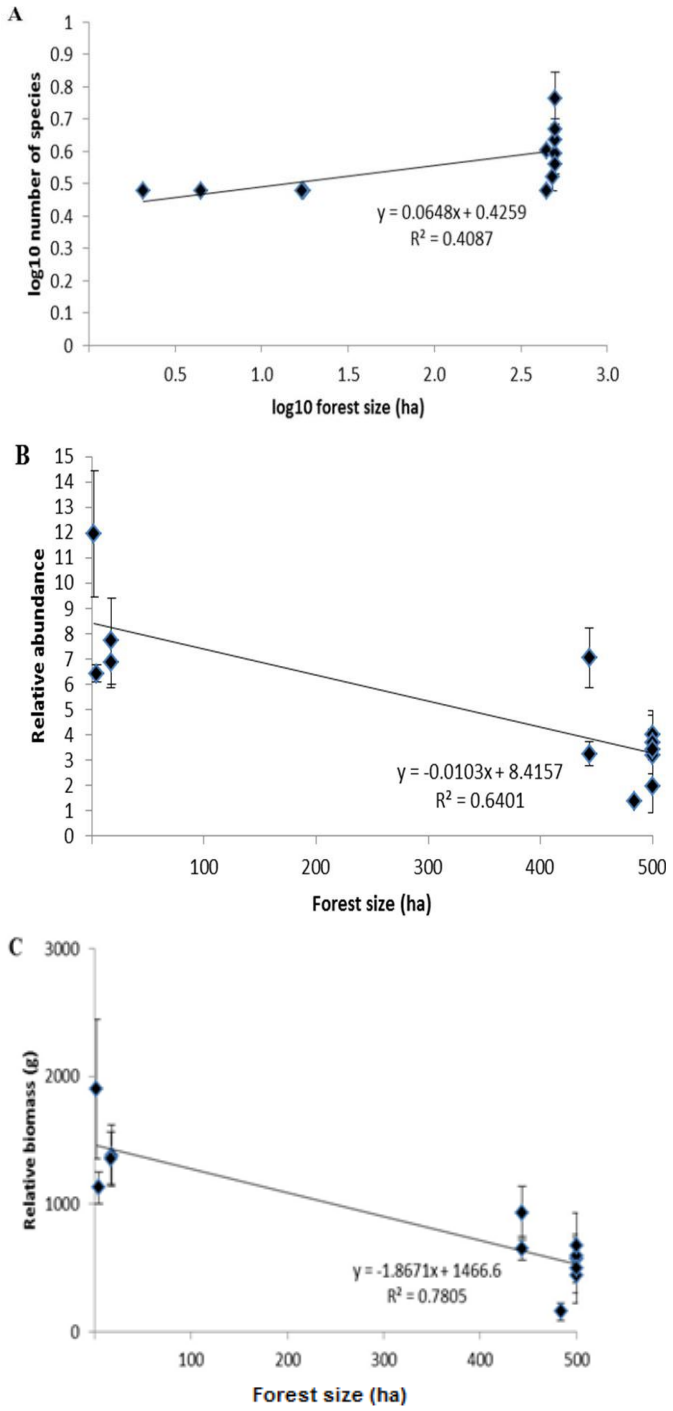

Figure 4. Correlations between species richness, abundance and biomass of small mammals and forest size. Mean ± 1 SD for (**A**) log10 number of species trapped, (**B**) relative abundance (mean number of individuals trapped per 100 station nights), and (**C**) relative biomass (total weight 9g) of all individuals trapped per 100 station nights).

In addition, displacement and loss of native forest species from fragmented forests due to the invasion of generalist species caused the decline in species richness in Brunei.[10] Extinction of native forest species in fragmented forests also occurred in Brazil[7,9,13] and Thailand.[62] These patterns were consistent with this study where loss of rare species and native forest species was observed in fragmented forests.

Reduced forest area in fragmented forests may contribute to the decreased species richness. Larger areas are able to accommodate more individuals because more physical space and resources are available.[72] Thus, larger areas allow the coexistence of ecologically similar species.[72] For example, the co-occurrence of *T. picta*, *T. tana*, *T. longipes* and *T. gracilis*, in this study were only recorded in all undisturbed forests and disturbed forest D4 but did not occur in fragmented forests. Some species, especially those with specific requirements are more vulnerable to the effects of fragmentation and forest disturbance.[73,74] For example, the comparatively large-bodies *Leopoldamys sabanus* (long-tailed giant rat) which requires large home ranges to survive[10] was absent in fragmented forests in this study. A similar pattern was seen in Thailand.[16]

Distance effects may also help explain the low species richness in fragmented forests in comparison with disturbed and undisturbed forests. Increased distance from source areas acts as a barrier to dispersal which prevents the immigration of new individuals.[12] In this study, fragmented forests were located further from continuous, pristine forests and were isolated by roads and a matrix of open savannah consisting of shrubs, scattered trees, and lalang grasses that appears unable to regenerate into kerangas forest. Roads and large clearings were found to pose barriers to dispersal of the *Maxomys rajah*,[63] and other species.[64,65] The geographical distance

separating these areas may explain why the study sites in Brunei-Muara have lower species richness compared with those in Tutong.

Another interesting point we found is that there were differences in species composition between the disturbed forests in Brunei-Muara (D1 and D2) and Tutong (D3 and D4). The time since disturbance may explain the differences between the disturbed sites. The disturbed forests in Brunei-Muara were recently subjected to repeated forest fires whereas the disturbed forests in Tutong were clear felled 40–50 yrs prior to this study.

Jones & Schmitz[66] found that the average recovery time for animal community after disturbance (logging) is over 40 yr. Thus, the small mammal communities in Tutong may have recovered from disturbance. This may also explain why the species compositions in D3 and D4 were similar to the undisturbed forests. Fragmented forests had the highest pooled abundance and biomass of small mammals compared with disturbed and undisturbed forests. This has been reported for small mammal communities in the fragmented and continuous forests of Amazonia.[67,68] In addition, the current study found a negative correlation of forest size on relative abundance and biomass of small mammals in kerangas forest. Previous studies have reported an increase in small mammal abundance and biomass with decreasing size of fragmented forests in Amazonia,[68] Brazil,[7] Brunei,[10] and Venezuela.[51] They highlighted that edge-induced habitat changes and an increase in individuals from the secondary habitats surrounding the forest fragments were the reasons for the increase in abundance and biomass.

One possible factor contributing to the high abundance and biomass of small mammals in fragmented forests is release from top-down control from predators.[45] Predators limit population growth. Fragmented forests, however, typically have depauperate predator communities.[75] For example, six species of predators including *Prionailurus bengalensis* (leopard cat) and *Viverra tangalunga* (Malay civet) were recorded in the undisturbed forests but were absent in fragmented forests in Brunei as determined by cage and camera trapping.[10] Thus, the removal or absence of predators would lead to increased densities of their prey—in this case, increased small mammal abundance. In Brazil, densities of the opossum *Didelphis marsupialis* increased due to fewer predators in small fragmented forests.[68]

Forest fragmentation could also enhance favourable conditions for certain small mammals and thus increase their abundance and biomass.[69] Edge-induced habitats such as habitats with decreased canopy cover and increased number of lianas lead to invasion by generalists that are better adapted to the fragmented forest environment.[70] In addition, there are greater opportunities and diversity of habitat in fragmented forests. For example, higher arthropod diversity and abundance and increased quantities of fallen timber due to edge effects have resulted in increased small mammal populations in fragmented Amazonian forests.[68] Here, the dominance of the three species (*S. muelleri*, *T. minor* and *C. notatus*) was observed in fragmented forests. Dominance of certain species over other co-occurring species was also observed in other fragmented forests.[10,16,51]

We found kerangas forests were rather species poor with a maximum of six species in a single undisturbed forest. Similar results were obtained by Charles and Ang[10] with eight species. Studies in primary dipterocarp forests have recorded 18 and 19 species in Brunei[71] and Sabah[29], respectively. This may reflect the actual low species numbers in kerangas forests. Similar patterns were observed in bird communities on Borneo.[40] However, the methods used could affect this result. Species caught were limited to omnivores and frugivores; other species with different diets, such as the bark-eating pygmy squirrel were not included. Future research could apply other methods to effectively capture different species to see if the same results are found especially species which are more relevant in regard to conservation issues. Another

limitation of the study is that it was not possible to distinguish the effects of fragmentation and forest disturbance on small mammals because of the nested study design. It would be ideal to partition the different drivers of species occurrence and subsequent changes in animal assemblages as part of the experimental design. Other aspects of the landscape context of the forest, such as presence or absence of corridors, shape of fragments, may also be of interest in future work.

Acknowledgements

Field work was supported by many and we thank Roberto Ignacio (John), Yadi, Simmons bin Benalai, Eyad Samhan bin Nyawa, Nurul Hafizah Adilah, Ishlah Rahman, Siti Norashikin, Hanyrol Ahmadsah, Ireni Sufinah, Catherine Liew, Hafizh Khalid, Khairuddin Khalid, Nanihasrinah Hanafi, Zolkepli Hj Ibrahim, Ahmat Ihkwan, Yanti, Anis, Hasnah, Fendi, Kholodin, Joe K. Charles and Ang Bee Biaw. We also thank the Forestry Department, Brunei, for the permission to conduct research in Andulau and Berakas Forest Reserves, as well as the Universiti Brunei Darussalam for permits and financial support (UBD/GSR/S&T/12). S.K. was supported by Universiti Brunei Darussalam's Graduate Research Scholarship.

References

[1] W. F. Laurance, H. L. Vaconselos and T. E. Lovejoy, *Oryx*, **2000**, 34, 39-45.

[2] L. Fahrig, *Annu. Rev. Ecol. Evol. Syst*., **2003**, 34, 487-515.

[3] F. Taubert, R. Fischer, J. Groeneveld, S. Lehmann, M. S. Müller, E. Rödig, T. Wiegand and A. Huth, *Nature*, **2018**, 554, 519–522.

[4] N. S. Sodhi, L. P. Koh, B. W. Brook and P. K. L. Ng, *Trends Ecol. Evol*., **2004**, 19, 654-660.

[5] N. S. Sodhi, M. R. C. Posa, T. M. Lee, D. Bickford, L. P. Koh, and B. W. Brook, *Biodivers. Conserv.*, **2010**, 19, 317-328.

[6] J. E. Bryan, P. L. Shearman, G. P. Asner, D. E. Knapp, G. Aoro, and B. Lokes, *PLoS ONE*, **2013**, 8, 1-7.

[7] R. Pardini, *Biodivers. Conserv*. **2004**, 13, 2567-2586.

[8] J. K. Charles and B. B. Ang, Brunei Darussalam: a collection of essays in conjunction with the 20th anniversary of University Brunei Darussalam, Ed. A. Ahmad, **2006**.

[9] E. B. V. De Castro and F. A. S. Fernandez, *Biol. Conserv.*, **2004**, 119, 73-80.

[10] J. K. Charles and B. B. Ang, *Biodivers. Conserv*., **2010,** 19, 543-561.

[11] A. B. Shadbolt and R. Ragai, *Biodivers. Conserv*., **2010,** 19, 531-541.

[12] R. H. MacArthur and E. O. Wilson, The Theory of Island Biogeography, **1967**, Princeton University Press, Princeton, NJ.

[13] R. Pardini, S. M. De Souza, R. Braga-Neto and J. P. Metzger, *Biol. Conserv*., **2005**, 124, 253-266.

[14] C. E. Dustan and B. J. Fox, *J. Biogeogr*., **1996**, 23, 187-201.

[15] S. M. Goodman and D. Rakotondravony, *J. Zool.*, **2000**, 250, 193-200.

[16] A. J. Lynam and I. Billick, *Biol. Conserv*., **1999**, 91, 191-200.

[17] S. Benedick, J. K. Hill, N. Mustaffa, V. K. Chey, M. Maryati, J. B. Searle, M. Schilthuizen and K. C. Hamer, *J. Appl. Ecol*., **2006**, 43, 967-977.

[18] S. Benedick, T. A. White, J. B. Searle, K. C. Hamer, N. Mustaffa, C. V. Khen, M. Mohamed, M. Schilthuizen and J. K. Hill, *J. Trop. Ecol*., **2007**, 23, 623-634.

[19] J. K. Hill, M. A. Gray, C. V. Khen, S. Benedick, N. Tawatao and K. C. Hamer, *Philos. Trans. R. Soc. Lond. B Biol. Sci*, **2011**, 366, 3265-3276.

[20] C. A. Bruhl, T. Eltz and K. E. Linsenmair, *Biodivers. Conserv*., **2003**, 12, 1371-1389.

[21] O. Konopik, C. L. Gray, T. U. Grafe, I. Steffan-Dewenter and T. M. Fayle, *Global Ecology and Conservation*, **2014**, 2, 385-394.

[22] A. Floren,. T. Muller, C. Deeleman-Reinhold and K. E. Linsenmair, *Ecotropica*, **2011**, 17, 15-26.

[23] F. R. Lambert and N. J. Collar, *Forktail*, **2002**, 18, 127-146.

[24] J. K. Hill, M. A. Gray, C. V. Khen, S. Benedick, N. Tawatao and K. C. Hamer, *Philos. Trans. R. Soc. Lond. B Biol. Sci*., **2011**, 366, 3265-3276.
[25] M. Nakagawa, H. Miguchi and T. Nakashizuka, *For. Ecol. Manage*, **2006**, 231, 55-62.
[26] H. Bernard, E. L. Baking, A. J. Giordano, O. R. Wearn, and A. H. Ahmad, *Mammal Study*, **2014**, 39, 141-154.
[27] K. T. Tanako, M. Nakagawa, T. Itioka, K. Kishimoto-Yamada, S. Yamashita, H. O. Tanaka, D. Fukuda, H. Nagamasu, M. Ichikawa, Y. Kato, K. Momose, T. Nakasjizuka and S. Sakai, Social-Ecological Systems in Transition Global Environmental Studies, Ed. S. Sakai, and C. Umetsu, **2014**, 24, Springer, Japan.
[28] H. Bernard, *Nat. Hum. Activities*, **2004**, 8, 1-11.
[29] K. Wells, Impacts of rainforest logging on non-volant small mammal assemblages in Borneo, *PhD Thesis*, **2005**, Universitat Ulm, Germany.
[30] K. Wells, M. Pferiffer, M. B. Lakim, and E. K. V. Kalko, *J. Anim. Ecol*., **2006**, 75, 1212-1223.
[31] K. Wells, E. K. V. Kalko, M. B. Lakim and M. Pfeiffer, *J. Biogeogr.*, **2007**, 34, 1087-1099.
[32] K. Wells, M. B. Lakim and M. Pfeiffer, *Ecotropica*, **2008**, 14, 113-120.
[33] K. Wells, E. K. V. Kalko, M. B. Lakim and M. Pfeiffer, *J. Mammal*, **2008**, 89, 712-720.
[34] H. Bernard, J. Fjeldsa and M. Mohamed, *Mammal Study*, **2009,** 34, 85-96.
[35] J. Cusack, Characterising small mammal responses to tropical forest loss and degradation in Northern Borneo using capture-mark-recapture methods, *Masters Thesis*, **2011**, Imperial College London, United Kingdom.
[36] J. Cusack, O. R. Wearn, H. Bernard and R. M. Ewers, *J. Trop. Ecol.,* **2014**, 31, 25-35.
[37] I. M. Turner, P. W. Lucas, P. Becker, S. C. Wong, J. W. H. Yong, M. F. Choong, and M. T. Tyree, *Biotropica*, **2000**, 32, 53-61.
[38] FRA. Global Forest Resources Assessment, **2010**, Forestry Department, Brunei Darussalam.
[39] O. O. Osunkoya, F. E. Othman and R. S. Kahar, *Ecological Research*, **2005**, 20, 205-214.
[40] I. A. Woxvoldm and R. A. Noske, *Forktail*, **2011**, 27, 39-54.
[41] C. L. Puan, A. W. Goldizen, M. Zakaria, M. N. Hafidzi and G. S. Baxter, *J. Raptor Res.,* **2011**, 45, 71-78.
[42] R. Rajaratnam, M. Sunquist, L. Raharatnam and L. Ambu, *J. Trop. Ecol*., **2007**, 23, 209-217.
[43] L. H. Emmons, *Am. Nat*., **1991**, 138, 642-649.
[44] M. Shanaham and S. G. Compton, *Biotropica*, **2000**, 32, 759-764.
[45] J. Terborgh, L. Lopez, V. P. Nunez, M. Rao, G. Shabuddin, G. Orihuela, M. Riveros, R. Ascanio, G. H. Adler, T. D. Lambert and L. Balbas, *Science*, **2001**, 294, 1923-1926.
[46] K. Wells, and R. Bagchi, *Raffles Bull. Zool.*, **2005**, 53, 281-286.
[47] K. Wells, R. T. Corlett, M. B. Lakim, E. K. V. Kalko and M. Pfeiffer, *J. Trop. Ecol.*, **2009**, 25, 555-558.
[48] B. G. Petticrew and R. M. F. S. Sadlier, *Can. J. Zool.*, **1970**, 48, 385-389.
[49] Q. Phillipps and K. Phillipps, Phillipps' Field Guide to the mammals of Borneo and their ecology, **2016**, Natural History Publications (Borneo), Kota Kinabalu, Malaysia.
[50] R. S. Sikes and the Animal Care and Use Committee of the American Society of Mammalogists, *J. Mammalogy*, **2016,** 663.
[51] T. D. Lambert, G. H. Adler, C. M. Riveros, L. Lopez, R. Ascanio and J. Terborgh, *J. Zool*., **2003**, 260, 179-187.
[52] D. M. Scott, C. B. Joyce and N. G. Burnside, *Estonian Journal of Ecology*, **2008**, 57, 279-295.
[53] R. K. Colwell and J. A. Coddington, *Philos. Trans. R. Soc. Lond. B. Biol. Sci.*, **1994**, 345, 101-118.
[54] A. E. Magurran, Measuring Biological Diversity, **2004**, Blackwell, Oxford, UK.

[55] J. Hortal, P. A. Borges and C. Gaspar, *J. Anim. Ecol*., **2006**, 75, 274-287.
[56] P. A. Henderson and R. M. H. Seaby, Species Diversity and Richness, **2001**, Pisces Conservation Ltd, UK.
[57] IBM Corp, IBM SPSS Statistics for Windows, **2011**, Armonk, New York.
[58] B. McCune and M. J. Mefford, Multivariate Analysis of Ecological Data, **2011**, Gleneden Beach, Oregon, USA.
[59] K. Wells, M. B. Lakim and R. B. O'Hara, *Biodivers. Conserv*., **2014**, 23, 2289-2303.
[60] IUCN, http://www.iucnredlist.org, **2017**.
[61] J. L. Mena and R. A. Medellin, *Mamm. Biol*., **2010**, 75, 83-91.
[62] L. Gibson, A. J. Lynam, C. J. A. Bradshaw, F. He, D. P. Bickford, D. S. Woodruff, S. Bumrungsi and W. F. Laurance, *Science*, **2013**, 341, 1508-1510.
[63] A. B. Shadbolt and R. Ragai, *Biodivers. Conserv*., **2010,** 19, 531-541.
[64] A. Rico, P. Kindlmann and F. Sedlacek, *Folia Zool*., **2007**, 56, 1-12.
[65] R. L. McGregor, D. J. Bender and L. Fahrig, *J. Appl. Ecol*., **2008**, 45, 117-123.
[66] H.P. Jones and O. J. Schmitz, *PLoS ONE*, **2009**, e5653.
[67] R. O. Bierregaard Jr, T. E. Lovejoy, V. Kapos, A. A. D. Santos and R. W. Hutchings, *BioScience*, **1999,** 42, 859-866.
[68] J. R. Malcolm, Tropical forest remnants: ecology, management and conservation of fragmented communities, Ed. W. F. Laurance, and R. O. Bierregaard, **1997**, 207, University of Chicago Press, Chicago, Illinois, USA.
[69] M. Saito and F. Koike, *PLoS One*, **2013,** e65464.
[70] T. D. Lambert, J. R. Malcolm and B. L. Zimmerman, *J. Mammal*., **2006,** 87, 766-776.
[71] J. K. Charles, Tropical rainforest research-current issues, Ed. D. S. Edwards, W. E. Booth, and S. C. Choy, **1996**, 175, Kluwer Academic Publishers, Dordrecht, Netherlands.
[72] T. W. Schoener, *Science*, **1974**, 185, 27-39.
[73] K. Henle, K. F. Davies, M. Kleyer, C. Margues and J. Settele, *Biodivers. Conserv*., **2004**, 13, 207-251.
[74] I. M. Turner, *J. Applied Ecology*, **1996**, 33, 200-209.
[75] A. G. Chiarello, *Biodivers. Conserv*., **1999**, 89, 71-82.

Gastropod diversity at Pulau Punyit and the nearby shoreline – a reflection of Brunei's vulnerable rocky intertidal communities

David J. Marshall[1], Azmi Aminuddin[1] and Pg Saimon Pg Hj Ahmad[1]*

[1]Environmental and Life Sciences, Faculty of Science, Universiti Brunei Darussalam, Jalan Tungku Link, Gadong, BE1410, Brunei Darussalam

**corresponding author email: david.marshall@ubd.edu.bn*

Abstract

Pulau Punyit (PPUN), a small islet on the South China Sea coastline of Brunei Darussalam, represents a significant portion of the country's natural rocky-shore ecosystem. We carried out a rapid survey of the intertidal gastropod species richness at PPUN, and compared this with species richness at other nearby natural and artificial rocky shores [Tungku Punyit (TPUN), Pantai Jerudong (PJER), Jerudong Park Medical Centre (JPMC) and Pantai Tungku (TUNK)]. A total of thirty two (32) species were collected from all of the shores. Species richness was greatest at the two natural shores studied (numbering 21 and 22 species at PPUN and TPUN, respectively), while the artificial shores were relatively depauperate. The natural shores however differed in species composition, abundance and body size of gastropods. These attributes varied with shore height, and appeared to relate to height-specific differences in abiotic stresses at the shores - at PPUN the high-shore is more exposed to the wind and sun, whereas at TPUN the mid-shore experiences greater sedimentation and mainland acidic seepage. Faunistic differences between the artificial and natural shores (Bray-Curtis similarity analysis) seemingly associate more closely with degree of habitat availability and abiotic stress than with shore proximity. We conclude that the country's rocky intertidal biodiversity, as reflected by the gastropod diversity, is mainly constituted by the natural rocky shore system. Because this is spatially constrained and vulnerable to locality-specific environmental stresses, this diversity is threatened and deserving of greater protection status.

Index Terms: gastropods, intertidal zone, marine diversity, rocky shores, species richness, tropical

1. Introduction

Intertidal ecosystems generally support significant biodiversity and provide several key ecosystem functions and services. While the shores of Brunei Darussalam comprise extensive intertidal soft benthic systems (sandy beaches, mudflats and mangroves), the country's natural hard intertidal rocky-shores are highly restricted in surface area (estimated to be less than 1 ha during spring low tide). The natural rocky intertidal ecosystem along the South China Sea coastline is largely limited to two small offshore islets, Pulau Punyit (***Figure 1A***) and Pelong Rocks, and their associated headlands at Tungku Punyit and Tanjung Batu, respectively. However, during the last decade, Tanjung Batu (near Muara) has experienced net sedimentation and has largely reverted to a sandy beach. More recently, this headland has been developed as a plan to limit erosion and establish a recreational facility. Public access to Tungku Punyit, which fringes the Empire Hotel and Country Club, is however restricted. Although artificial rocky promontories and bays have been constructed over other large tracts of the sandy beach coastline in the Brunei-Maura region (***Figure 1B***), these rocky systems are limited in habitat diversity (with the absence of platforms, intertidal pools, etc.) and apparently support depauperate intertidal biotas (DJM, personal observation).

(***A***)

(***B***)

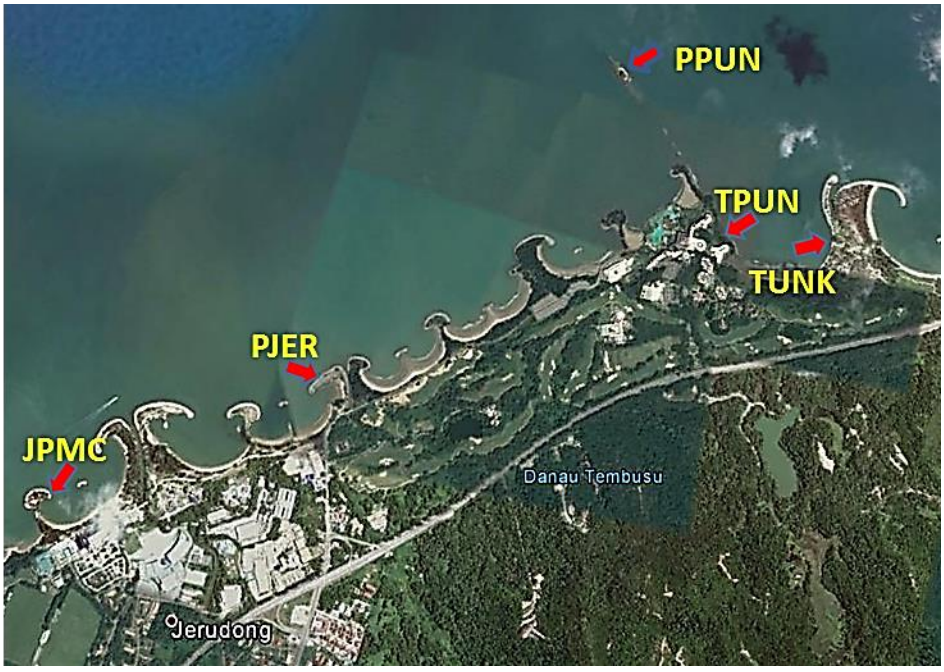

Figure 1. (***A***) Pulau Punyit viewed from a north-west aspect showing a steeply sloping rocky intertidal platform in the foreground. (***B***) Map indicating localities used in the gastropod faunistic survey. Pulau Punyit (PPUN), Tungku Punyit (TPUN), Pantai Tungku (TUNK), Pantai Jerudong (PJER) and Jerudong Park Medical Centre (JPMC)

Agbayani et al.[1] recognised the 'near-pristine' nature of Pulau Punyit (PPUN) and recommended protection status. Their report was followed by a survey of the islet's flora and fauna, which documented the occurrence and abundance of intertidal species, as well as the terrestrial species above the supralittoral zone.[2] Our knowledge of the country's gastropod fauna and its ecological significance has improved recently from studies using Brunei gastropods as a model system to understand physiological adaptation and ectothermic vulnerability to climate change.[3-6] This work has revealed inconsistencies in the gastropod species recorded at PPUN[2] and those from the nearby Tungku Punyit[7], prompting a rapid survey at PPUN. Here we report the findings of this survey. We further compare the PPUN gastropod assemblage with assemblages at Tungku Punyit (TPUN) and three nearby artificial rocky promontories at Pantai Jerudong (PJER), Jerudong Park Medical Centre (JPMC), and the far-south-west rocky headland of Pantai Tungku (TUNK)[7] (see ***Figure 1***).

2. Approach

The survey at PPUN (4.975N, 114.849E) was carried out during spring low tide (0.1m chart datum, CD; 7am to 9am) on 15 December 2016. Two biologists scanned and collected specimens of gastropods over a 2 h period (see ***Figure 1***). Observations and ad hoc collections of gastropods at other nearby localities (TPUN, 4.968N 114.855E; PJER, 4.958N 114.839E; JPMC, 4.951N 114.820E; TUNK 4.969N 114.859E; ***Figure 1***) were made over several preceding years.[3,4,6,7] Specimens were returned to the laboratory and were fixed and preserved in 70% ethanol. Reference specimens are housed in the UBD Museum (UBDM). Species were identified using several sources including Dharma (2005),[8] and species lists were compiled in MS-Excel. On the assumption that our records are representative of the taxa at each site, we undertook comparative diversity analyses. Diversity indices and a Bray-Curtis cluster analysis, to assess relationships among the assemblages, were computed using Primer, ver. 6.1.15. Species collected at PPUN, but currently not known at the other sites, or other species collected within the study area that are missing from the current existing photographic record,[7] were photographed using a Canon EOS digital camera (see ***Figures 4*** and ***5***).

3. Results and Discussion

A total of thirty two (32) rocky intertidal gastropod species were recorded during this study. Twenty one (21) species occurred at Pulau Punyit (PPUN), seven of which were not found elsewhere (see ***Table 1***). Species richness and diversity indicies of PPUN and the nearby natural shore at TPUN were comparable, though assemblages (species composition) differed between these localities for different shore levels (see ***Table 1***). PPUN showed a greater species richness in the mid to low shore, with *Cypraea arabica*, *Conus coronatus* and Columbellidae (5 spp.) recorded only there, whereas TPUN exhibited a more diverse high shore assemblage, with more Littorinidae and Neritidae species. These assemblage differences are likely influenced by multiple environmental factors, including more extensive low-shore rocky platforms and habitat availability at PPUN, and acidic water drainage and greater sedimentation loads at TPUN. Deposition of suspended sediment, originating from the Baram River (Miri) during the south west monsoon (more severe) and from the Brunei Bay during the north east monsoon season (less severe) potentially influences the assemblage structure at TPUN by smothering of the rock surfaces and constraining algal regrowth. The most susceptible species to sedimentation appeared to be *Monodonta* sp., *Batillaria* sp. and *Nerita albicilla* and *N. undata*, whereas *N. chamaeleon* and the higher-shore *N. polita* seemingly avoid or better tolerate the effects of sedimentation. The more rapidly circulating water current system and shoreline topography at PPUN are probably reasons for reduced sedimentation there. However, the high-shore habitat at PPUN is more exposed to solar radiation and wind than that at TPUN, where the littorinid assemblage is enhanced by coastal trees overhanging the upper shore.

Although quantitative data are unavailable, clear numerically-dominant genera at both PPUN and TPUN were *Planaxis* and *Nerita*, with species abundances varying obviously between these localities. Whereas *N. undata* is abundant at PPUN (see also Booth et al. 1997), it is currently rare at TPUN, with the population presumably recovering from sedimentation effects. High abundance of *Trochus cariniferus* in the low to subtidal zone at TPUN probably relates to preferred habitat there, including habitat created by a closely-associated grazing sea urchin. Snail body sizes varied conspicuously between the localities, such that most species at PPUN were larger (see ***Figure 2***). This suggests greater organismal fitness, apparently due to more optimal environmental water and food availability at PPUN; *N. albicilla* and *N. undata* at PPUN reached double the shell length of individuals occurring at TPUN, and the shell length of *N. chameleon* at TPUN was on average 75% that of snails at PPUN (see ***Figure 2***). An exception was observed in the high-shore where only minute individuals of *Echinolittorina malaccana* were collected at PPUN, reflecting

greater solar and wind exposure stress in this shore zone.

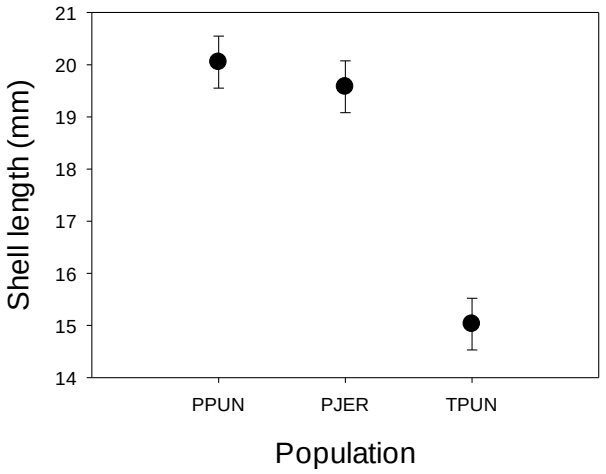

Figure 2. Mean (±95% CI) shell length of 30 randomly collected *Nerita chamaeleon* snails from each of PPUN, PJER and TPUN (see ***Figure 1*** for locality abbreviations).

When comparing natural and artificial rocky shores, the data confirm an impoverished diversity associated with the artificial shores (see ***Table 2***). Nonetheless, some species found on the artificial shores were not found, or were vastly less abundant, on the natural shores. Among the artificial sites, the diversity at PJER was greater than at the other shores; the outcrop at PJER gave rise to additional habitat, a sheltered (from wave action) habitat in a small bay. Acmeid limpets (*Notoacmea* sp.) were abundant in this sheltered bay, though absent from exposed and natural shorelines. Additionally, the muricids, *Rheshia bitubercularis*, and especially *Semiricinula tissoti* were common on the artificial piers but absent from PPUN, suggesting that they are out-competed at PPUN by their larger relative, *Mancinella echinulata*.

Relationships among the assemblages suggested a stronger influence by available habitat at a locality rather than by the locality's proximity to a more diverse natural rocky shore (see ***Figure 3***). The assemblage occurring at the artificial Pantai Tungku (TUNK), which was closest to the natural rocky ridge (PPUN and TPUN), was < 40% similar to the natural shores, whereas that at the more distant PJER showed 55% similarity (see ***Figure 3***). TUNK is clearly exposed to greater wave action, wind, sun and falls steeply to the sandy bottom with little extension of the lower shore zone. Furthermore, the PJER assemblage more closely associates with the natural rocky shore than with the other artificial shore at JPMC, which is around 60% similar to TUNK.

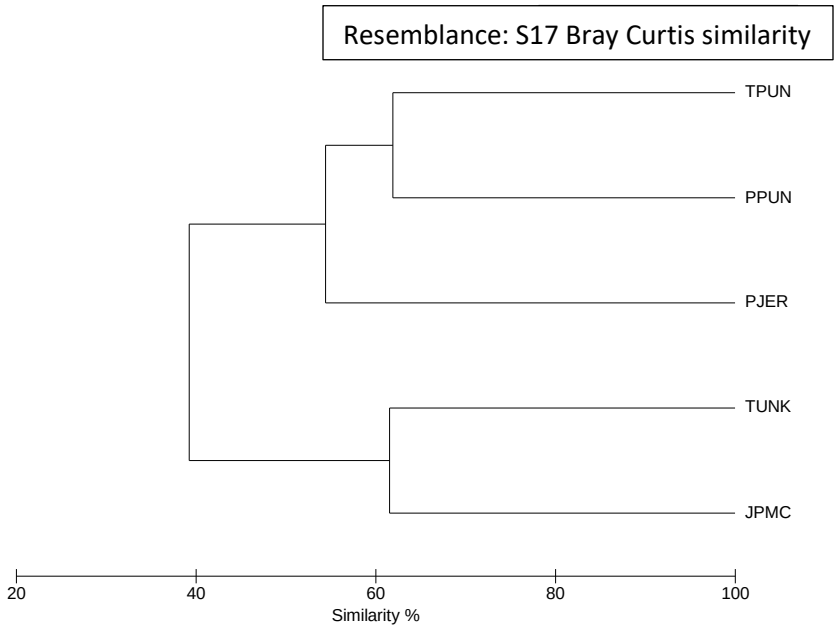

Figure 3. Bray Curtis similarity analysis showing faunistic associations across localities (see ***Figure 1*** for locality abbreviations).

4. Conclusion

Here we present the first dedicated (though preliminary) survey of the rocky-shore gastropods along the South China Sea coastline of Brunei Darussalam (excluding Brunei Bay), as a proxy for the country's intertidal hard-substratum, open-shore biodiversity. Essentially, this fauna - which typically dominates taxonomically and functionally in rocky intertidal systems - is depauperate and variable among natural and artificial shores. It appears fully constituted in the natural systems - in other words artificial shores only slightly enhance the diversity through the creation of more and novel habitat. Given the overall spatial constraint of the natural rocky shores in the region, there is a need for in-depth surveying and monitoring of key benthic taxa (algae, polychaetes, crustaceans, molluscs and echinoderms), as well as the implementation of a management and conservation plan.

Figure 4. Snail species collected at PPUN and not found at the other localities (A-G), as well as new photographic records of rocky shore littorinids from TPUN (H-J). A,Columbellidae sp. 1 (12); B, *Euplica scripta* (14); C, *Pictocolumbella ocellata* (15); D, Columbellidae sp. 2 (17); E, *Mancinella echinulate* (28); F,*Conus coronatus* (28); G, *Cypraea arabica* (39); H, *Echinolittorina melanacme* (7); I, *Littoraria sp*.(12); J, *Littoraria carinifera* (13). Number in parenthesis indicates shell length (mm).

Table 1. List of gastropod species recorded at Pulau Punyit and nearby natural (nat) and artificial (art) rocky shores (1=present, 0= absent)

		PPUN nat	TPUN nat	PJER art	JPMC art	TUNK art	Total
Species	**Family**						
Cellana testudinaria	Nacellidae	1	1	1	1	1	**5**
Notoacmea sp.	Acmaeidae	0	0	1	0	0	**1**
Patelloida saccharina	Acmaeidae	0	1	1	0	0	**2**
Monodonta canalifera	Trochidae	1	1	0	1	0	**3**
Trochus cariniferus	Trochidae	1	1	1	1	0	**4**
Angaria delphinus	Angariidae	0	1	0	0	0	**1**
Turbo intercostalis	Turbinidae	1	1	1	0	0	**3**
Nerita chamaeleon	Neritidae	1	1	1	0	0	**3**
Nerita albicilla	Neritidae	1	1	0	0	0	**2**
Nerita undata	Neritidae	1	1	0	0	0	**2**
Nerita polita	Neritidae	1	1	0	0	0	**2**
Nerita insculpta	Neritidae	0	1	0	0	0	**1**
Batillaria sp.	Batillariidae	1	1	0	0	0	**2**
Planaxis sulcatus	Planaxidae	1	1	1	0	0	**3**
Cypraea arabica	Cypraeidae	1	0	0	0	0	**1**
Echinolittorina malaccana	Littorinidae	1	1	1	1	1	**5**
Echinolittorina vidua	Littorinidae	1	1	1	1	1	**5**
Echinolittorina melanacme	Littorinidae	0	1	1	1	0	**3**
Littoraria undulata	Littorinidae	0	1	0	1	0	**2**
Littoraria carinifera	Littorinidae	0	1	0	0	0	**1**
Litoraria unid.	Littorinidae	0	1	0	0	0	**1**
Pictocolumbella ocellata	Columbellidae	1	0	0	0	0	**1**
Euplica scripta	Columbellidae	1	0	0	0	0	**1**
Columbellidae sp 1	Columbellidae	1	0	0	0	0	**1**
Columbellidae sp. 2	Columbellidae	1	0	0	0	0	**1**
Conus coronatus	Conidae	1	0	0	0	0	**1**
Semiricinula tissoti	Muricidae	0	1	0	1	1	**3**
Reishia bitubercularis	Muricidae	0	1	0	0	1	**2**
Morula sp.	Muricidae	1	1	1	0	0	**3**
Mancinella echinulata	Muricidae	1	0	0	0	0	**1**
Siphonaria atra	Siphonaridae	0	0	1	0	0	**1**
Siphonaria javanica	Siphonaridae	1	0	1	0	0	**2**
Total		**21**	**22**	**13**	**8**	**5**	

Table 2. Univariate species diversity indices.

Sample	S	N	d	J'	Brillouin	Fisher	H'(loge)	1-Lambda'
PPUN	20	20	6.342	1	2.117	****	2.996	1
TPUN	22	22	6.794	1	2.203	****	3.091	1
PJER	12	12	4.427	1	1.666	****	2.485	1
JPMC	8	8	3.366	1	1.326	****	2.079	1
TUNK	5	5	2.485	1	0.9575	****	1.609	1

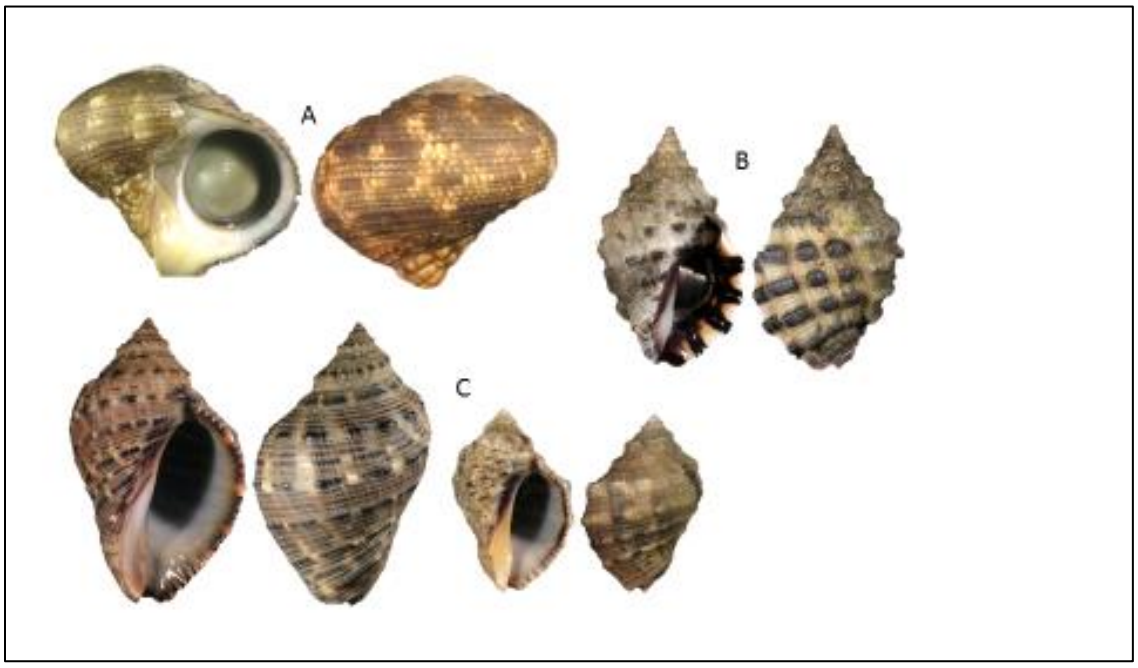

Figure 5. Recent snail species collected within the study area not included in the study and not previously given in photographic record for Brunei. A, *Lunella cinerea* (Born, 1778) (TPUN, 21); B. *Morula* sp. (Pantai Tungku, 16); C, *Purpura panama* (Röding, 1798) (Pantai Tungku, 34). Number in parenthesis indicates shell length (mm).

References

[1] C.V. Agbayani, M.W.R.N. De Silva, and M. Jayn, Island management strategy for Brunei Darussalam, **1992**, ICLARM Conference.

[2] W.E. Booth, K.M. Wong, A.S. Kamariah, S. Choy and I. Das I., *Sandakania*, **1997**, 9, 55-66.

[3] D.J. Marshall, Y. Dong , C.D. McQuaid and G.A. Williams, *J. Exp. Biol*., **2011**, 214, 3649–3657.

[4] D.J. Marshall, N. Baharuddin, E. Rezende and B. Helmuth, *Ecology and Evolution*, **2015**, 5, 5905-5919.

[5] S. Proum, C.D. Harley, M.C. Steele and D.J. Marshall, *Marine Biology*, **2017**, 164, 97.

[6] C. Monaco, C.D. McQuaid and D.J. Marshall, *Oecologia*, **2017**, 185 (4), 583-593.

[7] N. Baharuddin and D.J. Marshall, Common aquatic gastropods of Brunei, **2014**, Education and Technology Centre, Universiti Brunei Darussalam, Brunei Darussalam.

[8] B. Dharma, Recent and fossil Indonesian shells, **2005**, ConchBooks, Germany.

Bacterial community diversity associated with blood cockle (*Anadara granosa*) in Penang, Malaysia

Kamarul Zaman Zarkasi[1], Koh Fu Sheng[1], Teh Faridah Nazari[1], Nurfitri Amir Muhammad[1] and Amirul Al-Ashraf Abdullah[1]*

[1]School of Biological Sciences, Universiti Sains Malaysia, 11800 USM, Penang, Malaysia

**corresponding author email: kamarul.zarkasi@gmail.com*

Abstract

Bacterial communities of blood cockles (*Anadara granosa*) collected from wet market across Penang, Malaysia, were examined using a cultivation method. This study aimed to describe the major abundance of blood cockle bacteria and its relationship with different sampling locations. 16S rRNA gene analysis and culturable bacterial numbers were found to be slightly different between samples in two different locations potentially due to management, handling, transport and storage practices by the farmers, distributors and retailers. Results from this study indicated that most of bacteria found were typically present in blood cockles. The results revealed that there were slight similarities between sampling times; and slight differences on bacterial numbers between two different sampling locations. Based on the results, the blood cockle microbial communities comprised of members of the genera *Klebsiella* and *Bacillus*, which are greatly predominant, with highly dynamic of bacterial communities. Other bacterial genera found were *E.coli, Vibrio, Pseudomonas, Staphylococcus* and *Micrococcus*. The overall data demonstrated dynamic bacterial communities in blood cockles (*Anadara granosa*) and its diversity.

Index Terms: blood cockle; characterisation; bacterial community; diversity

1. Introduction

Marine and estuarine environments contain diverse microbial communities, such as *Vibrio* spp., *Pseudomonas* spp., *Klebsiella* spp., *Bacillus* spp., and *Aliivibrio* spp.[1-3] Most of the microbial species in blood cockles are allochtonous since blood cockles consume the surrounding water and are exposed to marine environments where those microorganisms are present.[2,3] The presence of certain pathogenic microorganisms are of concern; since it may be a health risk to consumers, and could be an indication of faecal pollutions. Blood cockle illnesses were previously reported due to contamination of *Vibrio vulnificus, E.coli* and *Vibrio parahaemolyticus*.[2-4] Human infections with *V. parahaemoiyticus* are usually linked to raw or mishandled seafood consumption[5] and is an important agent of human gastroenteritis. Despite that, there is high incidence and distribution variability in different regions, depending on the seasons,[1,2] pollution,[6] faecal pollution,[1,2] storage[1,2] and handling,[1,2] and management practices.[1,2] Hence, most strains of environmental and seafood isolates are likely to be virulent.[2] Understanding blood cockle microbiota and its influences can potentially lead to the improvements of sampling, storage, management practices and blood cockle farming, thus aiding in industrial sustainability. It was found that blood cockle microbial communities are highly dynamic[1-3] and sensitive to environmental and management factors[2].

The aim of this study is to investigate the microbial communities associated with blood cockles (*Anadara granosa*) and potential factors that influence the communities, such as environment, storage, handling, management practices, sampling time and location. The

primary question being asked, what is the main dominant of microbial communities associated with blood cockle (*Anadara granosa*) and the pathogenic microbes found from the blood cockles.

2. Experimental approach

2.1 Samples collection

Blood cockle samples were collected in October and December 2015 from wet markets in Bayan Baru and Relau, Penang, and only blood cockles from Penang's coastal/marine farms source were chosen. In this study, the samples are referred to as 'BB' (samples collected from Bayan Baru) and 'RL' (samples collected from Relau). Around 12 samples per sampling location (in total 24 samples) were randomly collected, and transported in a chilling ice box immediately to the laboratory. Blood cockle samples were examined thoroughly, their colour, smell and gross appearance recorded.

2.2 Microbial enumeration

The blood cockle samples were grouped into two different groups according to their sampling location (BB and RL). The samples were then cleaned with a brush under running tap water to remove any sand, debris and mud on the blood cockle's shell. Then the raw blood cockle were aseptically shucked using a sterile knife with intact bodies and liquor placed and pooled into a sterilized filter blender bag. The bag was massaged through by hand for one minute to separate the excess shell from the liquor and intact bodies. Then, the samples were transferred into a new full filter blender bag to remove remaining shells. A liquor of 3% sea salt peptone water (around 450ml) was added and homogenised for two minutes.[7,8] Samples (5 mL) were taken and processed for microbial enumeration and DNA extraction respectively. Serial dilutions were performed, and spread onto three types of agar media; Brain-Heart Infusion (BHI) Agar with 3% Sea salt (for detecting pathogenic bacteria of fungi), Marine Agar with 3% sea salt (for detecting marine microbes) and thiosulfate-citrate-bile salts-sucrose (TCBS) agar. Plates were incubated at 20°C for 24-72 hours. The Thiosulfate-Citrate Bile salts-Sucrose (TCBS) agar by Oxoid was also used in this research for detecting and checking any of *Vibrio* spp. growth which are normally associated with marine organisms.[9] After 24-72 hours of incubation, all plates were read and examined by standard plate count method. One loop of suspected growing colony was then streaked onto the agar and various media (using same type of agar) and incubated to get a pure colony for characterisation and identification (Gram-staining, microscopic observations of cellular morphology, colonial characteristics, biochemical tests and 16S rRNA gene analysis). In total, 60 colonies were chosen for identification.

2.3 Microbial identification

Representative colonies were transferred onto new plates and later identified using a commercial identification kit of API 20E 25 Strips (bioMerieux USA, St. Louis, MO, US) by following the manufacturer's instructions and standard protocols. All isolated colonies were reconfirmed using Gram-staining examination for bacterial cell morphology and series of biochemical tests (tested for Indole, MRVP, nitrate reduction, citrate test and lactose, sucrose and dextrose test). 16S rRNA gene analysis were also applied.

2.4 DNA extraction and 16S rRNA gene analysis from pure cultures

A single colony from a pure culture were transferred into Eppendorf tubes containing sterile distilled water and heated to 70°C for 10 minutes and centrifuged (4000 x g, 1 min). PCR was then performed using 2 µl of the heat extract with final concentrations of the PCR reaction mix including 1 µl (20 pmol) of each of primers 341F (5' CTA CGG GAG GCA GCA G) and 907R primer (5' AAA CTC AAA GGA ATT GAC) (GeneWorks, Australia),[10] 1 µl of bovine serum albumin, 12.5 µl of ImmoMix (Bioline, UK), and 7.5 µl of sterile distilled water to a final volume of 25 µl. Thermocycling was performed using a C1000 Thermal Cycle (Bio-Rad, California, United States) at 95°C for 10 minutes, 94°C for 1 minute, 55°C for 1 minutes, 72°C for 1 minutes,

repeated for 23 cycles; 72°C for 10 minutes, and soaking at 15°C.[10] The purified amplicons were then sequenced using an ABI 3730 automated sequencer using the Big Dye direct cycle sequencing kit. Comparison of individual rRNA gene sequences to those published in the BLAST database (http://blast.ncbi.nlm.nih.gov/) was done to determine the bacterial genera.

2.5 Statistical analysis

PRIMER6 and PERMANOVA+ (Primer-E, Ivybridge, UK) respectively were used to conduct analysis of variance (ANOVA) and Multidimensional scaling (MDS) to assess the influence of different factors on community compositions. The ANOVA derived significance values were considered significant when $P < 0.01$, while $0.01 < P < 0.05$ were considered marginally significant.[10,11]

3. Results and Discussion

3.1 Culturable bacterial population structure

This study investigated and analysed the number of bacteria and bacterial genera group present in blood cockles (*Anandara granosa*) collected from wet markets in Penang, where the sources came from Penang coastal/estuaries area and blood cockle farms in Penang. We assumed that microbial communities in blood cockles would show dynamic presence as previously indicated in response to environmental factors, handling, storage and management practices.[1-3]

Average viable counts from MA, BHI and TCBS plates for the two different sampling location of BB and RL, and the different collecting months were varied. For samples collected on October; BB samples the average viable counts were 4.66 Log CFU/g on MA, 4.76 Log CFU/g on BHI and 3.53 Log CFU/g on TCBS, while RL samples the viable counts were 7.17 Log CFU/g on MA, 7.13 Log CFU/g on BHI and 3.56 Log CFU/g on TCBS (see ***Figure 1***). During the following months of December, the population of BB and RL were almost the same with previous months, the average viable counts for BB were 4.69 Log CFU/g on MA, 4.78 Log CFU/g on BHI and 3.49 Log CFU/g on TCBS, while for RL were 7.20 Log CFU/g on MA, 7.19 Log CFU/g on BHI and 3.50 Log CFU/g on TCBS (see ***Figure 1***).

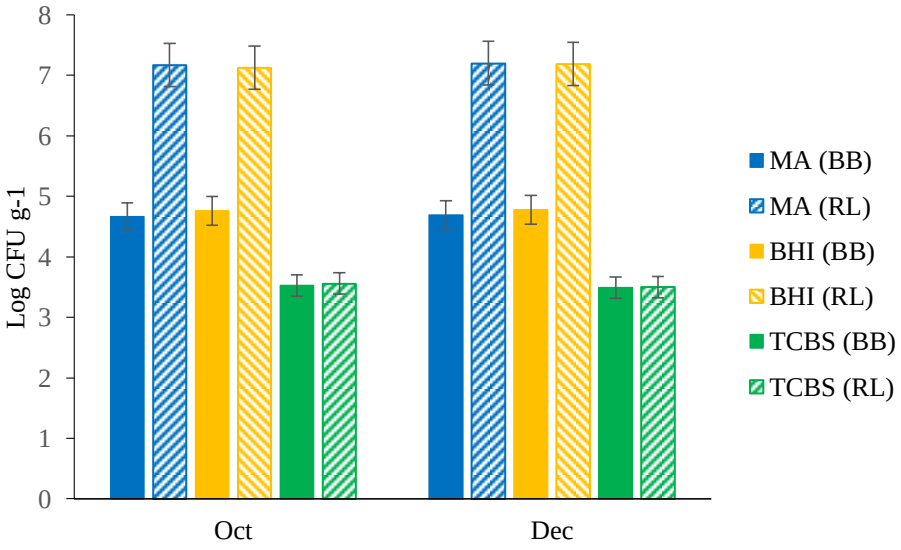

Figure 1. Total viable counts (TVC) populations for bacterial cultured from blood cockle (*Anadara granosa*) (n=12 for each location group) according to the time of sampling. TVC are derived from the colony numbers appearing on marine agar, BHI agar and TCBS agar.

3.2 Identification of blood cockle microbial communities

The results showed that the blood cockle bacteria were allocthonous, in which the dynamic influence was due to external and environmental factors.[11] The total 60 strains identified were dominated by bacterial groups belonging to the family *Enterobacteriaceae* (*Escherichia* and *Klebsiella*) making up >52% of total numbers), followed by the family of *Bacillaceae* (*Bacillus*), which made up >23% of total numbers (see ***Table 1***). The results are consistent among BB and RL samples, collected both in October and December (see ***Table 1***). The bacterial group belonging to the family of *Vibrionaceae* (*Vibrio* and *Aliivibrio*) were also identified, making up >7% of total numbers (see ***Table 1***).

Table 1. Relative abundances (in % of total numbers) of the most abundant microorganisms at family level associated with blood cockle.

Family	October		December	
	BB	**RL**	**BB**	**RL**
Enterobacteriaceae	51.7	53.3	50.0	51.7
Bacillaceae	23.3	25.0	21.7	23.3
Vibrionaceae	6.7	6.7	8.3	10.0
Staphylococcaceae	5.0	3.3	3.3	3.3
Pseudomonadaceae	5.0	3.3	3.3	1.7
Micrococcaceae	3.3	3.3	1.7	3.3
Other microorganisms	5.0	5.1	11.7	6.7

3.3 Microbial composition and diversity

Results indicated that the blood cockles (*Anadara granosa*) samples from BB and RL were dominated by the bacterial genera *Klebsiella* spp. and *Bacillus* spp., making up ~33% and ~23% of total number, respectively by morphological studies (see ***Table 2***) and 16S rRNA gene analysis (see ***Figure 2***). Other bacterial genera also found were *E.coli* (~18 % of total number), *Vibrio* spp. (~5 % of total number), *Staphylococcus* spp. (~3 % of total number), *Micrococcus* spp. (~3 % of total number) and *Pseudomonas* spp. (~3 % of total number) (see ***Table 2*** and ***Figure 2***), as visualised by the heat map (see ***Figure 2***). The results from October and December collection were similar and not significantly different. Results from the morphological and 16S rRNA gene sequences provide almost identical results, thus give conclusive evidence for bacterial identifications**.** The majority of identified bacterial genera from this study can be considered typically present in blood cockles and other marine animals.[10]

The high numbers of *Klebsiella* spp. and *Bacillus* spp., may indicate the influence of environmental factors and management practices in blood cockle farms, transportation and storage as well as conditions of the wet market. Farm management practices who are not control their workers movement, do not use treated water and clean their farms regularly might causes pathogenic contamination into their farm.[12,13] Beside, improper transportations and storage such as cockles are stored at warm temperature (not cold condition) could also cause contamination and spoilage.[13] Moreover, according to some researchers, these bacteria were easily found from blood cockles.[1,2] The presence of some bacterial species, such as *E.coli*, *Vibrio* spp., and *Staphylococcus* spp., could cause by the surrounding environments since the blood cockle farms and estuaries in Penang are known to be exposed to pollution from the industrial, residential and agriculture farms nearby.[1-3, 14,15]

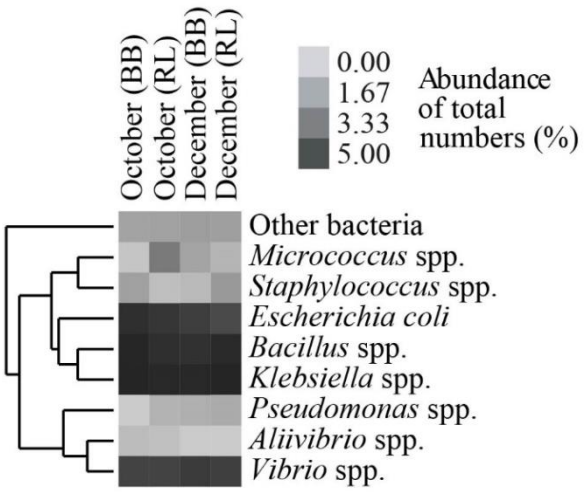

Figure 2. Heat map and hierarchical clustering plot of the blood cockle bacterial communities identified via 16S rRNA gene analysis.

The same bacterial genera were also detected from other marine organisms.[10,11,16] *E.coli*, *Staphylococcus* spp., and *Vibrio* spp., which are important because those bacteria can cause food spoilage and food-borne illnesses to blood cockle consumers. Frequent incidents were reported across the globe and raised concerned to the blood cockles consumptions.[17] Previous studies discussed the importance of the *Vibrio* and *Escherichia coli* in aquaculture and it presence in the aquaculture industry.[1-3,18-20] Both bacterial genera can be considered as an indicator for faecal pollution and may not be good to consume.

3.4 Analysis of variance (ANOVA) study of microbial diversity

The microbial community was influenced to a degree by location, management practices and environments according to the ANOVA analysis (see ***Figure 2***). Furthermore, the blood cockles from Penang coastal/estuaries are where knowingly affected by pollutants coming down from the industrial and residential estates as well as agriculture farms.[21] The different sampling locations produced an insignificantly different of analysis of variance (ANOVA) result ($P > 0.05$), moreover the interaction between sampling time was not significant too ($P = 0.11$), indicating bacterial diversity in this study was not influenced by the location and sampling time. Further analysis using pairwise tests showed that populations varied were not significant ($P > 0.05$). No separation was observed between the BB and RL ($P = 0.83$).

4. Conclusion

In this study, we described the predominant bacterial genera associated with blood cockles (*Anadara granosa*) are *Klebsiella* spp., and *Bacillus* spp., while others which commonly abundant were *E.coli*, *Vibrio* spp., *Pseudomonas* spp., *Staphylococcus* spp., and *Micrococcus* spp. Those abundant bacterial genera found in this study can be considered as typically isolated from the blood cockles and other marine animals[1-3,10] even though some of them could be of concern. The results obtained could be used to improve management strategies by the blood cockle farmers, distributors and retailers. Further studies on this topic is important to understand more about the bacterial communities associated with blood cockles and environmental factors that may shape bacterial diversity, especially in the tropic regions.

Acknowledgements

Thanks are extended to the Universiti Sains Malaysia (USM) for in-kind support and research funding (project 1001/PBlOLOGl/8011007). Thanks also extended to University Sains Malaysia staff for sampling help and advice.

Table 2. Identification of bacteria through biochemical characteristics.

Bacterial code	Indole	MR	VP	CU	NR	Lactose	Sucrose	Dextrose	Identified bacteria
BB1	+	+	-	-	+	+	+	+	*E.coli*
BB2	-	-	-	-	+	-	-	+	*Bacillus* sp.
BB3	-	+	-	+	+	+	+	+	*Klebsiella* sp.
BB4	-	-	-	-	+	-	-	+	*Bacillus* sp.
BB5	+	-	+		+	+	+	+	*Vibrio sp.*
BB6	-	+	-	+	+	+	+	+	*Klebsiella* sp.
BB7	-	+	-	-	+	+	+	+	*Staphylococcous* sp.
BB8	+	+	-	-	+	+	+	+	*E.coli*
BB9	+	+	-	-	+	+	+	+	*E.coli*
BB10	-	-	-	-	+	-	-	+	*Bacillus* sp.
BB11	-	+	-	+	+	+	+	+	*Klebsiella* sp.
BB13	-	+	-	+	+	+	+	+	*Klebsiella* sp.
BB14	-	-	-	-	+	-	-	+	*Bacillus* sp.
BB15	-	+	-	+	+	+	+	+	*Klebsiella* sp.
BB16	-	-	-	+	+	-	-	-	*Pseudomonas* sp.
BB17	-	+	-	+	+	+	+	+	*Klebsiella* sp.
BB18	+	+	-	-	+	+	+	+	*E.coli*
BB19	-	+	-	+	+	+	+	+	*Klebsiella* sp.
BB20	-	-	-	-	+	-	-	+	*Bacillus* sp.
BB21	+	+	-	-	+	+	+	+	*E.coli*
BB22	-	-	-	-	-	-	-	-	*Micrococcus* sp.
BB23	+	+	-	-	+	+	+	+	*E.coli*
BB25	-	-	-	-	+	-	-	+	*Bacillus* sp.
BB27	-	+	-	+	+	+	+	+	*Klebsiella* sp.
BB28	+	-	+		+	+	+	+	*Vibrio sp.*
BB29	-	+	-	+	+	+	+	+	*Klebsiella* sp.
RL1	+	+	-	-	+	+	+	+	*E.coli*
RL2	-	+	-	+	+	+	+	+	*Klebsiella* sp.
RL3	-	+	-	+	+	+	+	+	*Klebsiella* sp.
RL4	-	-	-	-	+	-	-	+	*Bacillus* sp.
RL5	-	-	-	+	+	-	-	-	*Pseudomonas* sp.
RL6	+	+	-	-	+	+	+	+	*E.coli*
RL7	-	-	-	-	+	-	-	+	*Bacillus* sp.
RL8	-	+	-	+	+	+	+	+	*Klebsiella* sp.
RL9	+	-	+		+	+	+	+	*Vibrio sp.*
RL10	-	-	-	-	-	-	-	-	*Micrococcus* sp.
RL11	-	+	-	+	+	+	+	+	*Klebsiella* sp.
RL12	-	-	-	-	+	-	-	+	*Bacillus* sp.
RL14	+	+	-	-	+	+	+	+	*E.coli*
RL15	-	+	-	+	+	+	+	+	*Klebsiella* sp.
RL17	-	-	-	-	+	-	-	+	*Bacillus* sp.
RL19	-	+	-	+	+	+	+	+	*Klebsiella* sp.
RL21	-	+	-	-	+	+	+	+	*Staphylococcous* sp.
RL22	+	+	-	-	+	+	+	+	*E.coli*
RL24	-	-	-	-	+	-	-	+	*Bacillus* sp.
RL25	+	-	+		+	+	+	+	*Vibrio sp.*
RL26	-	-	-	-	+	-	-	+	*Bacillus* sp.

RL27	-	+	-	+	+	+	+	+	*Klebsiella* sp.
RL28	-	-	-	-	+	-	-	+	*Bacillus* sp.
RL29	+	+	-	-	+	+	+	+	*E.coli*
RL30	-	+	-	+	+	+	+	+	*Klebsiella* sp.

References

[1] S. Areerat, Thai National AGRIS Centre, **2000**, Bangkok.

[2] K. Chowdhury, A. Jalal, M. Musa, *et al.*, *J. Biol. Sci.*, **2009**, 9, 841-850.

[3] J. Woodring, A. Srijan, P. Puripunyakom, *et al.*, *J. Food Prot.*, **2012**, 75, 41-47.

[4] B. L. Sarkar, R. Kumar, S. P. De and S. C. Pal, *Appl. Environ. Microbiol.*, **1987**, 53, 2696-2698.

[5] D. E. Johnson, F. M. Calia, D. M. Musher, *et al.*, *Humans J. Infect.*, **1984**, 150, 413-418.

[6] A. DePaola, L. A. Hopkins, J. T Peeler, *et al*., *Mar. Pollut. Bull.*, **1990**, 56, 2299-2302.

[7] T. A. Lorca, Virginia Polytechnic Institute and State University, **2000**, Blackburg.

[8] T. J. Green and A. C. Barnes, *J. Appl. Microbiol.*, **2010**, 109, 613–622.

[9] Y. Hara-Kudo, T. Nishina, H. Nakagawa, *et al.*, *Appl. Environ. Microbiol*., **2001**, 5819-5823.

[10] K. Z. Zarkasi, G. C. J. Abell, R. S. Taylor, e*t al., J. App. Microbiol.*, **2014,** 117, 18-27.

[11] K. Z. Zarkasi, R. S. Taylor, G. C. J Abell, *et al.*, *Microb. Ecol.*, **2016**, 71, 589–603.

[12] A. C. G. Heath, D. J. W. Cole, D. M. Bishop, *et al.*, *Vet. Parasitol.*, **1995**, 56, 239-254.

[13] D.F. Leavitt, USDA Risk Management Agency, **2009**, Raleigh.

[14] C. K. Yap, Y. Hatta, F. B. Edward, *et al.*, *Pertanika J. Trop. Agric. Sci.*, **2008**, 31, 205–215.

[15] D. R. Shahunthala, *Malay. Fish J.*, **2015**, 53-58.

[16] M. B. Hovda, B. T. Lunestad, R. Fontanillas, *et al.*, *Aquaculture*, **2007**, 272, 581-588.

[17] H. Urbanczyk, J. C. Ast, M. J. Higgins, *et al.*, *Int. J. Syst. Evol. Microbiol.*, **2007**, 57, 2823-2829.

[18] B. Austin, *Sci. World. J.*, **2006**, 6, 931-945.

[19] B. Austin and X. H. Zhang, *Lett. Appl. Microbiol.*, **2006**, 43, 119-124.

[20] C. T. Eng, J. N. Paw and F. Y Guarin, *Aquaculture*, **1989**, 20, 335-343.

[21] S. Khodami, M. Surif, W. O. Wan Maznah and R. Daryanabard, *Mar. Pollut. Bull.*, **2017**, 114, 615–622.

Seagrass diversity in Brunei Darussalam: first records of three species

Nadhirah Lamit[1], Yasuaki Tanaka[1] and Haji Mohamed Bin Abdul Majid[1,2]*

[1]Environmental and Life Sciences, Faculty of Science, Universiti Brunei Darussalam, Jalan Tungku Link, Gadong BE1410, Brunei Darussalam
[2]Rimba Ilmu, Universiti Malaya, Kuala Lumpur 50603, Malaysia

**corresponding author email: drahlamit@hotmail.com*

Abstract

Borneo is one of the regions expected to have the highest diversity of seagrasses in the world. However, the diversity of seagrasses has scarcely been studied in Brunei Darussalam. The diversity of seagrasses at the intertidal and subtidal zones in Brunei was extensively surveyed in 2016. Six species of seagrasses were found at Pulau Muara Besar and Pulau Bedukang, and this was the first time that three of them (*Halophila beccarii*, *Halodule pinifolia*, and *Cymodocea rotundata*) had been recorded in Brunei. The total area of seagrass distribution around the two islands was approximately 1.5 km^2. The present study extends the distribution of seagrasses on Borneo and suggests that Brunei has a rich seagrass diversity and an aquatic ecosystem supported by the seagrasses.

Index Terms: Borneo, Brunei Bay, seagrass, *Cymodocea rotundata* Asch. & Schweinf., *Halophila beccarii* Asch., *Halodule pinifolia* (Miki) Hartog

1. Introduction

Seagrasses are hydrophytic angiosperms also called marine flowering plants. The importance of seagrasses has been recognized from many perspectives.[1] A total of 72 seagrass species have been reported in the world, and the highest diversity lies in insular Southeast Asia and extends across tropical northern Australia.[2,3] Malaysia has reported the highest diversity of seagrasses (14-18 species) in Southeast Asia, along with the Philippines.[2-9] Borneo has 10-13 species,[6,7] suggesting that the island is one of the most suitable habitats for seagrasses in Asia. This high diversity of seagrasses in Borneo could occur partially because of its complex and diversified geographical structures.[4,5] However, most surveys on seagrass diversity and distribution on Borneo are still limited to Sabah, Malaysia, which is the most northern region of Borneo.[4,6,7]

Brunei Darussalam (hereafter, Brunei) is located on the northwest coast of Borneo and is surrounded by Sarawak, Malaysia (see ***Figure 1***). Though Brunei is expected to have a high diversity of seagrasses, no research article on seagrasses in Brunei is found in major international publications.[10] Four species (*Enhalus acoroides* (L.f) Royle, *Halophila ovalis* (R.Br.) Hook.J., *Halophila spinulosa* (R.Br.) Asch., and *Thalassia hemprichii* (Ehrenb. ex Solms) Asch. were recorded a long time ago, but their specific features and locations have never been described.[11,12] The purpose of this study is to evaluate the present seagrass diversity in Brunei and to develop the knowledge of the diversity and distribution of seagrasses in this region.

2. Materials and Methods

The coastline of Brunei was extensively surveyed by walking during low tide periods from March to October 2016. The survey sites include the coastal areas of Muara (MU), Meragang (ME), Jerudong (JE), Pulau Muara Besar (PMB), and Pulau Bedukang (PB) (see ***Figure 1***). PMB (5°00'N, 115°06'E) and PB (4°58'N, 115°03'E) are small, desolate islands on the Brunei side of

Brunei Bay and are covered with mangrove vegetation. The depth of the surveyed sites was <1.5 m from the mean surface level. Seagrass samples were collected by gently digging the sediment by hand to prevent breakage of the underground parts. Salinity and pH of the water at the collection site were also measured with a multiprobe device (556 MPS, YSI Inc., USA) on 31 August 2016.

After seagrass collection, the seagrasses were brought back to the laboratory of Universiti Brunei Darussalam (UBD) for identification and preservation. Seagrasses were thoroughly cleaned using freshwater and the morphology of each seagrass individual was carefully recorded and then identified according to the references.[13-15] Identified seagrasses were dried, sprayed with 5% formalin, and then pressed to preserve them in the Herbarium of the Faculty of Science, UBD (UBDH).

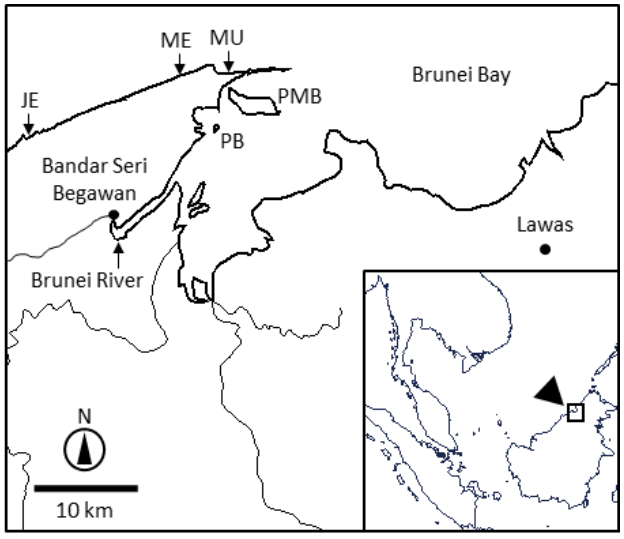

Figure 1. The locations of the survey sites: Pulau Muara Besar (PMB), Pulau Bedukang (PB), Muara (MU), Meragang (ME), and Jerudong (JE).

3. Results

A total of six seagrass species were recorded at PMB and PB (see ***Figure 2***): *Cymodocea rotundata* Asch. & Schweinf., *Enhalus acoroides* (L.f) Royle, *Halophila beccarii* Asch., *Halophila ovalis* (R.Br.) Hook.J., *Halodule pinifolia* (Miki) Hartog, and *Thalassia hemprichii* (Ehrenb. ex Solms) Asch. *E. acoroides, H. beccarii, H. ovalis*, and *T. hemprichii* are in the Hydrocharitaceae family. *C. rotundata* and *H. pinifolia* are in the Cymodoceaceae family.

3.1 Description

Halophila ovalis (R.Br.) Hook.J.

Common name: Spoon grass, dugong grass, paddle weed

The leaf blade is oval, 9−12 mm long and 5−7.5 mm wide. The leaf margin is smooth and without hairs on the leaf surface. There are 10−25 cross veins on the leaf blade, ascending at 45−60° from the mid-vein. A pair of leaves arises from each node, and the petiole is 10−20 mm long. The base of the petioles is covered by leaf scales. The rhizome is white, thin and smooth.

Halophila beccarii Asch.

Common name: Ocean turf grass

H. beccarii has 4 to 10 leaves arranged in a pseudowhorl. The leaf blade is lanceolate, 5−8 mm long and 0.9−1.6 mm wide. There are three longitudinal veins on the leaf blade. The petiole is 4−15 mm long. Each shoot carries a whorl of leaves. The whorl of leaves may arise from the erect shoot or rhizome. The base of the petioles is covered by scales. The rhizome is light-colored, thin and smooth.

Enhalus acoroides (L.f.) Royle

Common name: Tape seagrass

The leaf blade is linear, flat, 310 mm long and 11 mm wide. The leaf tip is rounded, and the leaf margin is thick and slightly inrolled. The rhizome is very thick, measuring up to 10 mm in diameter. The unique feature of this species is the presence of rolled leaves, cord-like roots and black bristles, which are located on the rhizome. Female flower bracts were observed in September 2016. The female flower bract emerged from a long, coiled stalk.

Thalassia hemprichii (Ehrenb. ex Solms) Asch.

Common name: Turtle grass

The leaf blade is sickle-shaped, 20−45 mm long and 4−5 mm wide. The leaf tip is rounded and smooth. The leaf blade has longitudinal veins with red bands of cells. No hairs are present on the leaf surface. The stem is short, erect and

holds 2−4 leaves from every shoot. The base of the shoot is covered by a fully enclosed leaf sheath. The rhizome has leaf scars, and the roots are thick.

Cymodocea rotundata Asch. & Schweinf.
Common name: Smooth ribbon seagrass
The leaf blade is linear and flat, 80−140 mm long and 2−4 mm wide. The leaf tip is rounded, and the leaf margin is slightly serrated. The leaf has longitudinal veins. Each shoot has 2−3 leaves, and the base of the leaves is covered with a rectangular leaf sheath. The rhizome is white and smooth.

Halodule pinifolia (Miki) Hartog
Common name: Needle seagrass
The leaf blade is linear, narrow and flat, 10−150 mm long and <1 mm wide. The leaf margin is smooth and finely serrated at the tip. The diagnostic feature of this species is the black central vein that splits into two at the leaf tip. The stem is short, erect, covered by a sheath and often has scars. Each shoot bears 1−2 leaves. The rhizome is pale-colored, thin, and smooth. The roots are thin (<1 mm).

3.2 Distribution
Four seagrass species (*H. ovalis*, *H. beccarii*, *C. rotundata*, *H. pinifolia*) were found at PMB, while five species (*H. ovalis*, *H. beccarii*, *E. acoroides*, *T. hemprichii*, *H. pinifolia*) were found at PB. *H. ovalis*, *H. beccarii*, *C. rotundata*, and *T. hemprichii* usually coexisted with *H. pinifolia* and those species were often found in the intertidal zone around the pneumatophores of mangrove trees on both islands. *H. pinifolia* was the most extensively distributed around both islands. *E. acoroides* was found only in the subtidal zone at PB and was away from the other seagrass species. The total area of seagrass distribution around PMB and PB was roughly estimated to be 1.5 km^2 from an aerial map. The salinity and pH of the water where the seagrasses were collected at PMB were 22.7 and 7.9, respectively. At PB, the salinity and pH of water were 20.7 and 7.7 respectively. No seagrass was found at the other surveyed coastal sites.

4. Discussion

In total, six species of seagrasses were found at PMB and PB, and this was the first time that three of them (*C. rotundata*, *H. beccarii*, *H. pinifolia*) had been recorded in Brunei. The Brunei coast has been thought unfavorable for seagrass growth[16] and in fact, no seagrass was found at the other surveyed sites in the present study. However, the present discovery of seagrasses at PMB and PB demonstrates that Brunei has an aquatic environment that is suitable for seagrasses. On the Malaysian side of Brunei Bay (Lawas, Sarawak), eight species of seagrasses have been recorded,[8] and six of them correspond to the species in Brunei. This shows that a similar diversity of seagrass is present on both Brunei and Malaysian sides of Brunei Bay. However, due to the geographical location of seagrasses in the Brunei side, which is more enclosed, higher impacts from terrestrial inputs, such as river waters, are expected. These impacts could lower salinity and pH in comparison to common seawater. However, seagrasses are euryhaline plants and are widely distributed in brackish waters around the world[17] and thus, the changes in salinity levels may have little effects on the seagrass diversity in Brunei. Since only intertidal and subtidal zones were surveyed in the present study, more seagrass species may be found in deeper zones in Brunei.

The seagrass beds at PMB and PB are located at the mouth of the Brunei River (see ***Figure 1***). Organic and inorganic soil particles had accumulated on the seagrass leaves, indicating that the seagrass bed is acting as a natural filter to trap particles from the overlying water and is reducing the discharge of turbid waters to offshore coral reefs.[18] The trapped organic matter would support the nutritional requirements of epiphytic organisms and lead to increased biodiversity of the estuarine ecosystem.[19] Moreover, some feeding trails of dugongs were observed at PMB while conducting the present study (data not shown). These findings emphasize the ecological and environmental importance of the seagrass beds in Brunei and highlight the necessity of further specific research in the future.

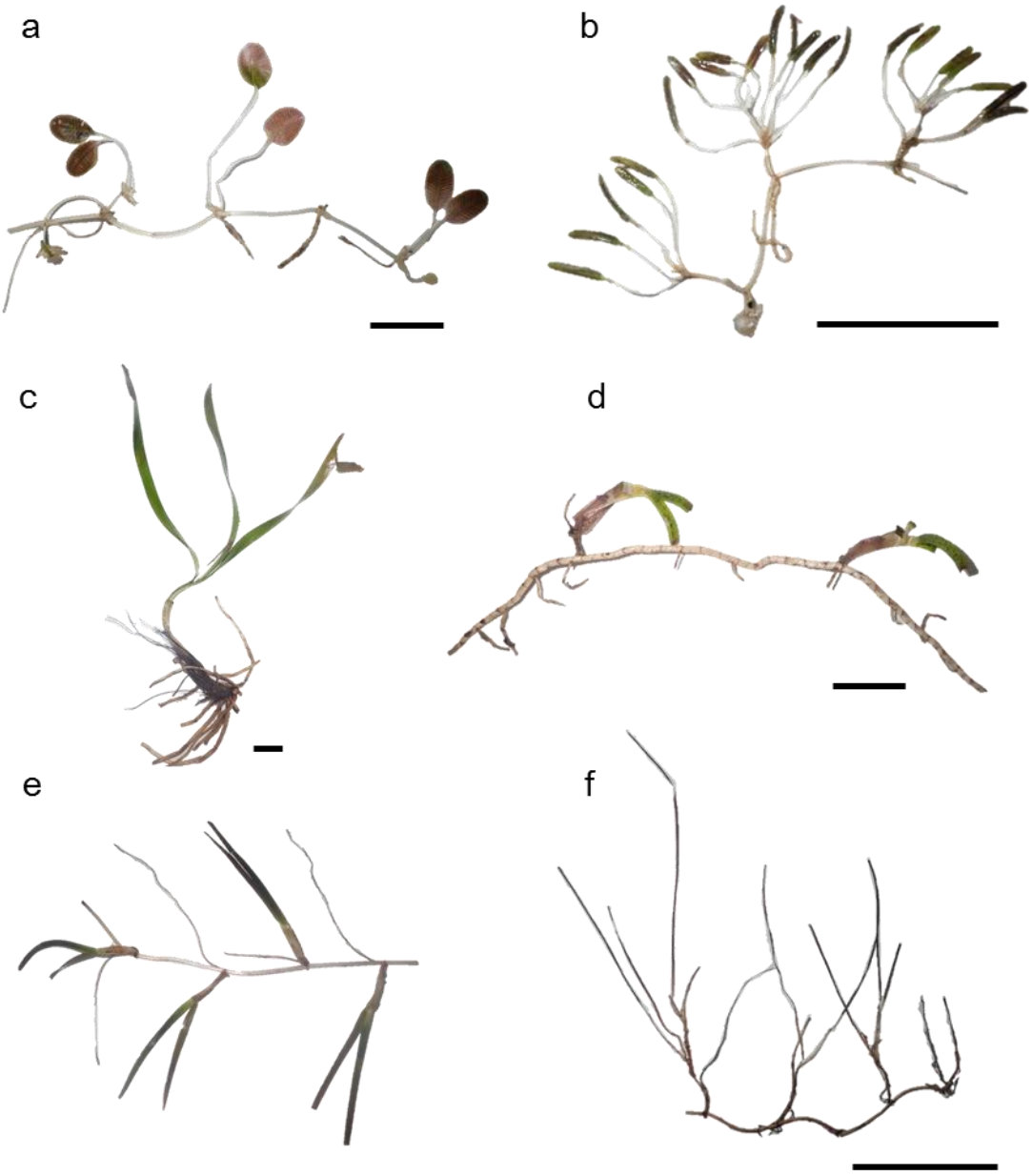

Figure 2. The seagrasses collected in Brunei Darussalam. (a) *Halophila ovalis*, (b) *Halophila beccarii*, (c) *Enhalus acoroides*, (d) *Thalassia hemprichii*, (e) *Cymodocea rotundata*, (f) *Halodule pinifolia*. Scale bar = 3 cm.

5. Conclusion

The first extensive surveys of seagrasses have been conducted along the coastline of Brunei in 2016, and six species, including three never previously recorded in Brunei, were found at PMB and PB in Brunei Bay. The present findings suggest that Brunei Bay has a rich seagrass diversity comparable to other regions in Southeast Asia and emphasizes the importance of taking action to conserve and monitor the seagrass community.

Acknowledgements

We are grateful to Dr. Muta Harah (Universiti Putra Malaysia) for the confirmation of seagrass identification, and to two anonymous reviewers whose many valuable comments helped to improve the article. This study was financially supported by the Competitive Research Grant (CRG) from Universiti Brunei Darussalam (UBD/OAVCRI/CRGWG(013)/170601).

References

[1] R. J. Orth, *et al.*, *BioScience*, **2006**, 56(12), 987−996.

[2] F. Short, *et al.*, *J. Exp. Mar. Biol. Ecol.*, **2007**, 350(1−2), 3−20.

[3] F. T. Short, *et al.*, *Biological Conservation*, **2011**, 144(7), 1961-1971.

[4] N. Ismail, *Pertanika J. Trop. Agric. Sci*, **1993**, 16(2), 111−118.

[5] V. C. Chong and A. Sasekumar, *Fisheries Science*, **2002**, 68(sup 1), 566−571.

[6] J. S. Bujang, *et al.*, *Aquatic Ecosystem Health and Management*, **2006**, 9(2), 203-214.

[7] K. Ibrahim, National Report on Seagrass of the South China Sea: Malaysia, **2008**, Department of Fisheries Malaysia.

[8] S. A. Jaaman, *et al.*, Report on UNEP/CMS Southeast Asia Regional Meeting on dugongs and workshop on developing standardized analysis protocols for dugong questionnaire survey project data for Southeast Asia region, **2011**, CMS.

[9] S. M. Yaakub, *et al.*, *Nature in Singapore*, **2013**, 6, 105−111.

[10] J. L. S. Ooi, *et al.*, *Estuarine, Coastal and Shelf Science*, **2011**, 92(1), 118−131.

[11] C. den Hartog, The sea-grasses of the world, **1970**, Amsterdam: North-Holland Pub. Co.

[12] E. P. Green and F. T. Short, World Atlas of Seagrasses, **2003**, Cambridge: UNEP World Conservation Monitoring Centre.

[13] F. T. Short, *et al.*, Global Seagrass Research Method, **2001**, Elsevier.

[14] AlgaeBase, **2017**, World-wide electronic publication, National University of Ireland, Galway. http://www.algaebase.org [Accessed 3 May 2017]

[15] Seagrass-Watch, **2017**. James Cook University, Cairns, Australia. http://www.seagrasswatch.org [Accessed 3 May 2017]

[16] L. M. Chou, *et al.*, The coastal environmental profile of Brunei Darussalam, **1987**, 43−57, Ministry of Development, Brunei Darussalam.

[17] K. Hillman, *et al.*, *Aquatic Botany*, **1995**, 51, 1.

[18] Y. Tanaka, *Scientia Bruneiana*, **2016**, 15, 13.

[19] M. B. Hossain and D. J. Marshall, *Aquatic Biosystems*, **2014**, 10, 11.

SCIENTIA BRUNEIANA

NOTES TO CONTRIBUTORS

Manuscript Submission and Specifications

Scientia Bruneiana is published twice a year. The deadline for submission of manuscripts is **30th June for the end of year edition** and the **31st December for the May edition**.

Manuscripts should be submitted to the Chief Editor, Dr. Abby Tan Chee Hong, Faculty of Science, UBD (abby.tan@ubd.edu.bn), in Microsoft Office Word (.DOCX) format.

Papers will be refereed prior to acceptance. Authors are welcome to suggest potential international referees.

Articles outlining original research findings as well as mini-review articles are welcomed. There are two special categories: "Brief Communications" and "Research Notes". Contributions to either category should be 300 to 1000 words long (no more than 3 pages in length). The "Research Notes" section is earmarked for summaries of the results and outcomes of projects receiving UBD Science Faculty research grants.

Manuscripts should be written in English (British or American). All manuscripts should be in 12pt Times New Roman, **single-spaced**, **single column** and A4 formatted (2cm margins from the edge).

Title page

The first page should include the title of the article, author's names and addresses of the institutions involved in the work. The paper title is only capitalized on proper nouns and the first letter. Latin, scientific genus and species should be italicized. The authors' affiliations are denoted with a superscripted number and the corresponding author denoted with a * at the end of the author's name. Only the corresponding author's email need to be listed.

Example format of the title page:

First record and conservation value of *Periophthalmus malaccensis* Eggert from Borneo

First Author[1], John H. Smith[2,3], Muhamad Ali Abdullah[2] and Siti Nurul Halimah Hj. Ahmad[1]*

[1]Environmental and Life Sciences, Faculty of Science, Universiti Brunei Darussalam, Jalan Tungku Link, Gadong, BE1410, Brunei Darussalam
[2]Department of Chemical Sciences, Faculty of Science, Universiti Brunei Darussalam, Jalan Tungku Link, Gadong, BE1410, Brunei Darussalam
[3]Department, University, Street Adress, Postcode, Country

**corresponding author email: corresponding.author@ubd.edu.bn*

Abstract Page and Index Terms

The second page of the manuscript should include the abstract (up to 300 words) and index terms (subject heading, or descriptor, in information retrieval, that captures the essence of the topic of a document).

Example format of the abstract and index terms page:

Abstract

The abstract is a self-contained description of the work in one paragraph of up to 300 words. It must include no references or foot notes, but it must describe the key points of the work. This should include

a description of the work that was done and why it was it done. It should include brief conclusions and any significant numerical findings such as derived constants or important parameters.

Index Terms: resolution, spectroscopy, microscopy

Main body of text

For original research articles, the main body of text of the manuscript should include the following appropriately numbered sections: **1. Introduction**, **2. Experimental approach**, **3. Results and Discussions** and **4. Conclusion** followed by **Acknowledgements**, **References** and **Appendices** (if necessary).

Each different numbered section may contain italicised subheadings which are numbered appropriately, e.g. *2.1*, *3.1*, etc.

Review articles will obviously not conform to this format. In the case of other submissions where the above format may be unsuitable, you are advised to contact the editor prior to submitting the article.

Reference to figures, tables and equations

The main body of text should not include figures and/or tables, but should refer to figures and tables. If a certain figure or table was not referred to in the main body of text then it will be considered irrelevant and therefore will not be included in the publication. When referring to a figure or table in the text, the words figure and/or table should be bold and italicized e.g. ***Figure 1*** and ***Table 1***. The words "figure" and "table" should be spelled out in full and not abbreviated. For further instructions on figures and tables (including dimensions, colour schemes and formats), please refer to the figures and tables section (below).

Equations could be displayed in-line or centred by itself, but must be accompanied by a number and individual terms/symbols explained. When When referring to the equation in the text, the word "Equation" should be bold and italicized e.g. ***Equation 1***. The words "Equation" should be spelled out in full and not abbreviated.

Example format of equation:

An example of an equation is shown for ***Equation 1***, Weber Morris intraparticle diffusion:

$$q_t = k_{id} t^{1/2} + C \qquad (1)$$

and Boyd model (***Equation 2***):

$$F = 1 - \frac{6}{\pi^2} exp(-B_t) \qquad (2)$$

where F = q_t / q_e, F is the fraction of solute adsorbed at any time, t and B_t is mathematical function of F.

In-line citation style

The in-line citation should be in IEEE referencing format (numbers with square brackets), generated using a reference manager. Example:

> Even though various studies have shown this [1]–[5], there are others that have contradicted this [6]–[10]. Data was obtained from [11].

Please note that brackets should go **before** punctuation.

References

The reference/bibligraphic list should only include references cited in the text and should be listed in the references section in the following format:

Journal article

[1] J. H. Surname and J. E. Doe, "Title," *Journal*, Vol., No., Pages, Year. DOI: (number)

Textbook/Chapter of a book
[2] J. H. Surname and J.E. Doe, *Title of Textbook*, Publication House, Year.

Dissertation/Thesis
[3] J.H. Surname, "Title of Thesis," University, Year

Webpages/Online Databases
[4] "Website/Database name/body," Year. Available: http;//www.weburl.com. [Accessed 18-Apr-2017]

These should be generated automatically if a reference manager software has been used. When there are **three or more authors**, just state the name of the first author, e.g. J. H. Surname, et. al. Please include the digital object identifier (DOI) for journal articles.

Figures and Tables

A list of tables, figures and captions should be given at the end of the manuscript after the reference list. These must be appropriately numbered in the order that they appear in the paper. Each table and figure must be adequately discussed and referenced in the text. It is important that you do not include tables and figures in the main body of text of your submitted manuscript.

Sizing

Please keep tables/figures/images/illustrations to have a **maximum width of either 8.4 cm (single column) or 17.5 cm (double column)**, with enough clarity that the images does not appear blurred, skewed or pixelated (unless the pixelation is unavoidable from the raw data collection).

Text

Texts in figures and tables should be 10pt, using either Times New Roman, Arial or Calibri font, with consistent font size and style throughout the manuscript's figures/tables/artwork/images/illustrations. Please ensure that texts do not fall below 8pt size as this will greatly affect readability of said text.

Colour

Colour images are highly encouraged for the on-line issue, however they should be designed such that the information is still obvious in grey-scale too for the print version.

Graphs

Graphs could either be saved as an embedded graph format in DOCX or as an image (JPEG or TIFF). Graphs should have clearly-labelled axes and lines that can be distinguished in both color for on-line and grey-scale for print version. You can use dotted and dashed lines etc, or you can use different data point types when appropriate to discriminate between data sets.

Tables

Tables could either be saved as an embedded table format in DOCX or as an image (JPEG or TIFF), with appropriate captions/titles.

Captions

All figures and tables should be appropriately captioned. The caption should be sufficiently able to explain the figure/table without the reader having to refer to the main text. The words "figure" and/or "table" should be bold. italicized and spelled out fully (not abbreviated), followed by a full stop (also bold and italicized). The rest of the caption should not be bold and italicized (unless it is a scientific genus or species).

Example format for figure/table caption:

> ***Figure 1.*** *Periophthalmus malaccensis* collected in Sungai Bunga, Brunei (UBDM MBu081013mal); a. freshly dead specimen, lateral view; b. live specimen; c. freshly dead specimen, ventral view, detail (scale bars are 10 mm long).

Manuscripts that do not conform to the above instructions will be returned without review.